THE JOURNAL OF BIOLOGICAL CHEMISTRY VOL. 289, NO. 33, pp. 22942–22957, August 15, 2014

The Unfolded Protein Response and the Phosphorylations of Activating Transcription Factor 2 in the *trans*-Activation of *il23a* Promoter Produced by β-Glucans*

Received for publication, September 26, 2013, and in revised form, June 23, 2014 Published, JBC Papers in Press, June 30, 2014, DOI 10.1074/jbc.M113.522656

Mario Rodríguez[‡], Esther Domingo[§], Sara Alonso[§], Javier García Frade[¶], José Eiros[‖], Mariano Sánchez Crespo[§1], and Nieves Fernández[‡]

From the [‡]Departamento de Bioquímica y Biología Molecular, Facultad de Medicina, Universidad de Valladolid, 47005-Valladolid, the [§]Instituto de Biología y Genética Molecular, Consejo Superior de Investigaciones Científicas, 47003-Valladolid, the [¶]Division of Hematology, Hospital Universitario Rio Hortega, 47012-Valladolid, and the [‖]Division of Microbiology, Hospital Universitario Rio Hortega, 47012-Valladolid, Spain

Background: Phagocytosis and Th17 immune response control fungal invasion.
Results: β-Glucans mobilize nuclear C/EBP homologous protein (CHOP) and increase activating transcription factor 2 (ATF2) binding to the *il23a* promoter.
Conclusion: β-Glucans direct proapoptotic CHOP to phagosomal vesicles and induce ATF2-dependent *il23a* transcription.
Significance: The mechanisms underlying the unfolded protein response and the *trans*-activation of *il23a* elicited by β-glucans are ascertained.

Current views on the control of IL-23 production focus on the regulation of *il23a*, the gene encoding IL-23 p19, by NF-κB in combination with other transcription factors. C/EBP homologous protein (CHOP), X2-Box-binding protein 1 (XBP1), activator protein 1 (AP1), SMAD, CCAAT/enhancer-binding protein (C/EBPβ), and cAMP-response element-binding protein (CREB) have been involved in response to LPS, but no data are available regarding the mechanism triggered by the fungal mimic and β-glucan-containing stimulus zymosan, which produces IL-23 and to a low extent the related cytokine IL-12 p70. Zymosan induced the mobilization of CHOP from the nuclear fractions to phagocytic vesicles. Hypha-forming *Candida* also induced the nuclear disappearance of CHOP. Assay of transcription factor binding to the *il23a* promoter showed an increase of Thr(P)-71–Thr(P)-69-activating transcription factor 2 (ATF2) binding in response to zymosan. PKC and PKA/mitogen- and stress-activated kinase inhibitors down-regulated Thr(P)-71–ATF2 binding to the *il23a* promoter and *il23a* mRNA expression. Consistent with the current concept of complementary phosphorylations on N-terminal Thr-71 and Thr-69 of ATF2 by ERK and p38 MAPK, MEK, and p38 MAPK inhibitors blunted Thr(P)-69–ATF2 binding. Knockdown of *atf2* mRNA with siRNA correlated with inhibition of *il23a* mRNA, but it did not affect the expression of *il12/23b* and *il10* mRNA. These data indicate the following: (i) zymosan decreases nuclear proapoptotic CHOP, most likely by promoting its accumulation in phagocytic vesicles; (ii) zymosan-induced *il23a* mRNA expression is best explained through coordinated κB- and ATF2-dependent transcription; and (iii) *il23a* expression relies on complementary phosphorylation of ATF2 on Thr-69 and Thr-71 dependent on PKC and MAPK activities.

Cytokines of the IL-12 family such as IL-12 p70 and IL-23 play a central role in the polarization of the immune response into the Th1 and Th17 types. Because both cytokines share a common chain, IL-12 p40 (encoded by the gene *il12/23b*), and differ in a specific chain for each cytokine, IL-12 p35 (gene *il12a*) for IL-12 p70 and IL-23 p19 (gene *il23a*) for IL-23, the regulation of the expression of these chains is central to the polarization of the immune response. NF-κB plays a role in the control of these cytokines, but other transcription factors are required for the selective regulation of each cytokine chain. The fungal surrogate zymosan, which is mainly composed of β-glucans, stands out as a strong stimulus for IL-23 production, although it inhibits the expression of IL-12 p70 induced by the LPS/TLR4 route (1, 2) through a mechanism involving the transcriptional repression of *il12a* (3, 4). These findings help explain the role of dectin-1, a C-type lectin-like β-glucan receptor, in the polarization of the immune response to the Th17 type during the infection by *Candida*, *Aspergillus*, and *Pneumocystis jirovecii*, because β-glucans are a major component of fungal cell wall. However, there is no mechanistic explanation for the high level of *il23a* expression elicited by β-glucans. Studies addressing the involvement of transcription factors other than NF-κB have pointed at activator protein 1 (AP1) (5), activating transcription factor 2 (ATF2) and SMAD family (6), CREB[2] and C/EBPβ (7), CHOP (8), and XBP1 (9), but these

* This work was supported by Plan Nacional de Salud y Farmacia Grant SAF2010-15070, Fundación Ramón Areces, Red Temática de Investigación Cardiovascular from Instituto de Salud Carlos III, and Junta de Castilla y León.

[1] To whom correspondence should be addressed: Instituto de Biología y Genética Molecular, C/Sanz y Forés 3, 47003-Valladolid, Spain. Tel.: 34-983-423273; Fax: 34-983-184800; E-mail: mscres@ibgm.uva.es.

[2] The abbreviations used are: CREB, cAMP-response element-binding protein; Ab, antibody; C/EBPβ, CCAAT/enhancer-binding protein; CHOP, C/EBP homologous protein; COX, cyclooxygenase/prostaglandin synthase; CRE, cAMP regulatory element; DC, dendritic cells; ddF, 1,9-dideoxyforskolin; ERS, endoplasmic reticulum stress; PERK, double-stranded RNA-activated protein kinase-like ER kinase; SIRT1, sirtuin 1; TBP, TATA-box binding protein; TLR, Toll-like receptors; UPR, unfolded protein response.

studies have been carried out mainly in murine cells by using bacterial LPS, virus, and TNFα as stimuli.

The involvement of CHOP and XBP1 is relevant because together with ATF6 these are the transcription factors associated with the endoplasmic reticulum stress (ERS)/unfolded protein response (UPR), and there is increasing evidence showing UPR-related molecules as integral elements of the transcriptional program controlled by innate immunity receptors (10). CHOP is a member of the C/EBP family of transcription factors that is activated in the cascade PERK/eIF2α/ATF4 in an attempt to control protein misfolding. If the resolution of the stress is not achieved, CHOP will trigger apoptosis. *XBP1* mRNA is translated into a functional protein after activation of the ribonuclease domain of inositol-requiring enzyme 1α (IRE1α) and excision of a 26-nucleotide unconventional intron from *XBP1* mRNA that causes a frameshift in the *XBP1* coding sequence resulting in the translation of the functional transcription factor. The UPR has been associated with the enhanced production of IL-23 in the pathogenesis of ankylosing spondylitis due to the accumulation of misfolded HLA-B27 heavy-chain homodimers in monocytes and lymphocytes (11, 12). In this study, we have carried out a comprehensive analysis of the mechanisms involved in the transcriptional regulation of *il23a* in human monocyte-derived dendritic cells (DC). Our results have disclosed the following: (i) a central role for ATF2 in the transcriptional regulation of *il23a* by zymosan, most likely related to the ability of the β-glucan receptor dectin-1 to activate protein kinases A, C, and MAPK; (ii) the disappearance of nuclear CHOP protein during the phagocytosis of zymosan and hypha forming *Candida* yeast by DC, thus suggesting that the disappearance of CHOP might be a mechanism to preserve phagocytic cells from the apoptosis associated with CHOP activity during fungal invasion but is not involved in IL-23 production.

EXPERIMENTAL PROCEDURES

Cells and Reagents—DC were obtained from human mononuclear cells collected from pooled buffy coats of healthy donors provided by Centro de Hemoterapia de Castilla y León. Each sample contained cells from five donors of the same ABO group system. The differentiation of monocytes was carried out by culture in the presence of GM-CSF (800 units/ml) and IL-4 (500 units/ml) for 5 days, and differentiation was assessed by immunofluorescence flow cytometry of CD40, CD80, CD83, CD86, CD11b, CD11c, and C-type lectin receptors. Zymosan from *Saccharomyces cerevisiae*, mannan, the β(1,3)-glucan curdlan from *Alcaligenes faecalis*, laminarin, carboxylated latex beads, SB203580, U0126, leptomycin B, and LPS were from Sigma. Depleted zymosan was purchased from InvivoGen (San Diego) or obtained by boiling zymosan for 1 h in 10 N NaOH and intensive washing. SRT1720 was from Cayman Chemical (Ann Arbor, MI). EX-527 was from Santa Cruz Biotechnology Inc. (Santa Cruz, CA). SP600125, bisindolylmaleimide I, H89, tunicamycin, and pustulan, a β(1,6)-glucan from *Umbilicaria pustulosa,* were from Calbiochem. Carboxylated latex beads were used for covalent coupling of laminarin and mannan with dicyclohexylcarbodiimide using the Neises-Steglich esterification reaction (13). *Candida albicans* (Cek1 strain) was provided by Dr. Jesús Pla from Universidad Complutense de Madrid, Spain. The α(1,3–1,6)-glucan nigeran from *Aspergillus niger* was a gift from Dr. Carlos R. Vázquez de Aldana and Francisco del Rey from Instituto de Biología Funcional y Genómica, Salamanca, Spain. The inhibitors of the endonuclease activity of IRE1α, MKC3946, and MKC8866 (14) were a gift from Dr. John Patterson, MannKind Corp., Valencia, CA.

Ethics Statement—This study was approved by the Bioethical Committee of the Spanish Council of Research (CSIC), and the written informed consent of all healthy donor subjects was obtained at Centro de Hemoterapia y Hemodonación de Castilla y León Biobank. The participants received written consent according to the regulations of the Biobank. The researchers received the samples in an anonymous way. The process is documented by the Biobank authority according to the specific Spanish regulations. The ethics committee approved this procedure before starting the study.

Laser-scanning Confocal Fluorescence Microscopy—DC were seeded on polylysine-coated glass coverslips for 12 h and then stimulated with zymosan particles. Cells were fixed with 10% formaldehyde in PBS and stained with anti-CHOP antibody (Ab) (Santa Cruz Biotechnology sc-793) and goat anti-rabbit IgG Ab labeled with Alexa-Fluor®480. The coverslips were observed by laser-scanning confocal fluorescence microscopy using a Leica TCS SP5 apparatus equipped with a white light laser and a Leica 63PL APO NA 1.40 oil immersion objective. Image analysis and subcellular colocalization fluorograms were generated and analyzed using a Leica confocal software package and ImageJ Fiji software (National Institutes of Health).

XBP1 Splicing Assay—This was carried out by RT-PCRs with primers spanning the unspliced regions. To address properly the spliced, unspliced, and heteroduplexes, gel electrophoresis was carried out in 3% agarose. When the purpose of the experiments was the quantification of the splicing, real time RT-PCR was carried out using an antisense primer overlapping the splice junctions (*sxbp1* AS primer in Table 1).

Immunoblots—Proteins were separated by electrophoresis in SDS-PAGE and transferred to nitrocellulose membranes. The membranes were used for the immunodetection of CHOP, phosphorylated form of eIF2α (InVitrogen 44728G), and ATF6 (Abcam ab11909). Histone H3 (Millipore 05-928) and TATA-box binding protein (TBP) (Diagenode TBPCSH-100) were used for protein load control. For immunoblots directed to assay nuclear proteins, the nuclear extracts were obtained by using a nuclear extract kit (Active Motif).

Real Time RT-PCR—Total RNA was obtained by TRIzol/chloroform extraction and used for RT reactions. Cycling conditions were adapted to each set of primers. The glyceraldehyde-3-phosphate dehydrogenase gene (*gapdh*) was used as a housekeeping gene to assess the relative abundance of the different mRNAs, using the comparative cycle threshold method. The procedure was used to assay *sXBP1*, *chop*, *il23a*, and *ptgs2* (the gene encoding COX-2) mRNA. The sequences of the primers are shown in Table 1.

Chromatin Immunoprecipitation (ChIP) Assay—ChIP assays were conducted with Ab against ATF2 (Santa Cruz Biotechnology sc-6233), P-ATF2 (Thr-71, Cell Signaling 9221), P-ATF2 (Thr-69, Abcam ab28848), ATF4 (Santa Cruz Biotechnology

TABLE 1
Primers used for ChIP and RT-PCRs
S indicates sense, and AS indicates antisense.

Promoter primers
il23a X2-Box/TRE S: 5′-CTC TAG CCA CAG CAA CCA CA-3′
il23a X2-Box/TRE AS: 5′-GCCCGCCCTTTATACCAGCA-3′
il23a CHOP-C/EBP proximal S: 5′-agAACTCCTGGGCTTCCTAGCCAT-3′
il23a CHOP-C/EBP proximal AS: 5′-GGCCTCATTCTGACGTCATCCA-3′
il23a CHOP-C/EBP distal S: 5′-TAACGGTTTAGGCCCAGCTGAC-3′
il23a CHOP-C/EBP distal AS: 5′-TGTTGCGTGGCAGGAACTACA-3′
il23a C/EBPβ S: 5′-TTCCCAGTTCTCCAAGTTCC-3′
il23a C/EBPβ AS: 5′-TTGATTCCTACCTGATGCCC-3′
il23a CRE S: 5′-AGACCTCCATTCAGGACAAG-3′
il23a CRE AS: 5′-TCGAAGACGTCAGAATGAGG-3′
il23a ATF2 S: 5′-CATTGCAAACAGCTCACCAT-3′
il23a ATF2 AS: 5′-ATTTCCTCACTTCCTCCTGC-3′
il12a control S: 5′-GCGAACATTTCGCTTTCATT-3′
il12a control AS: 5′-ACTTTCCCGGGACTCTGGT-3′
Coding sequence primers
chop S: 5′-GCAGAGATGGCAGCTGAGTC-3′
chop AS: 5′-AGCCAAGCCAGAGAAGCAGGGT-3′
xbp1 S: 5′-TAAGACAGCGCTTGGGGATGGA-3′
xbp1 AS: 5′-ATACCGCCAGAATCCATGGGGA-3′
sxbp1 AS: 5′-CTGCACCTGCTGCGGACTCA-3′
il23a S: 5′-CATGGGCCTTCATGCTATTT-3′
il23a AS: 5′-TTT GCATTG TCAGGTTTCCA-3′
ptgs2 S: 5′-CAATTGTCATACGACTTGCA-3′
*ptgs2*AS: 5′-GTGGGAACAGCAAGGATTTG-3′
atf2 S: 5′-CATTGCAAACAGCTCACCAT-3′
atf2 AS: 5′-ATTTCCTCACTTCCTCCTGC-3′
gapdh S: 5′-GTCAGTGGTGGACCTGACCT-3′
gapdh AS: 5′-AGGGGAGATTCAGTGTGGTG-3′

sc-200), ATF6, C/EBPβ (Santa Cruz Biotechnology sc-150), CHOP (Santa Cruz Biotechnology sc-793), CREB (Santa Cruz Biotechnology sc-186), P-CREB (Ser-133, Millipore 06-519), and XBP1 (BioLegend 647501) as reported previously (15). Briefly, cells were stimulated and then washed twice with PBS and fixed with 1% formaldehyde. Cross-linking was terminated by 0.125 M glycine. Crude nuclear extracts were collected by microcentrifugation and resuspended in a lysis buffer containing a high salt concentration. Chromatin sonication was carried out using a Bioruptor device from Diagenode (Liege, Belgium). The chromatin solution was precleared by adding protein A/G PLUS-agarose for 30 min at 4 °C under continuous rotation. After elimination of the beads, Ab was added for overnight incubation at 4 °C, and then protein A/G PLUS-agarose was added and incubated for an additional period of 2 h at 4 °C. Beads were harvested by centrifugation at 12,000 rpm and sequentially washed with lysis buffer high salt, wash buffer, and elution buffer. Cross-links were reversed by heating at 67 °C in a water bath, and the DNA bound to the beads was isolated by extraction with phenol/chloroform/isoamyl alcohol. Irrelevant Ab and sequences of the *il12a* promoter were used as control of binding specificity. Results are expressed as percentage of input.

Nucleofection Protocol—DC were transfected with the Amaxa™ human dendritic cell Nucleofector kit using the U-002 program in the Amaxa Nucleofector II system. Typical transfections used 2 million cells and 0.07 nmol of ON-TARGETplus human ATF2 or ON-TARGETplus nontargeting pool siRNA, in 0.1 ml of human DC Nucleofector solution. DC were nucleofected on the 3rd day of differentiation and used for the experiments 48 h later.

Statistical Analysis—Data are represented as the mean ± S.E. and were analyzed with the Prism 4.0 statistical program (GraphPad Software). Comparison between two experimental groups was carried out using the two-tailed Student's *t* test. Differences were considered significant for $p < 0.05$.

RESULTS

CHOP Disappears from Nuclear Extracts Following Zymosan Challenge—Zymosan is a particulate stimulus consistent with it being the cell wall of *S. cerevisiae*. On this basis, zymosan uptake poses energetic and space challenges to phagocytic cells that might require enhanced protein synthesis and put the cell at risk of ERS/UPR. Because previous studies suggested that CHOP and XBP1 are involved in *il23a trans*-activation, we posited the possible occurrence of the UPR in DC stimulated with zymosan. Unexpectedly, but in keeping with reports showing that CHOP protein expression has been detected in resting human monocytes (16) and that the UPR reaction seems to be required for the appropriate function of DC (17), we observed CHOP protein in the nuclear extracts of DC in the resting state (Fig. 1*A*). In contrast, CHOP could not be detected in the cytoplasm nor in whole cell lysates (data not shown), thus suggesting a preferential location of CHOP to the nucleus that probably explains the few studies reporting the presence of the protein in resting cells. Addition of different stimuli failed to show a definite increase of CHOP protein in the nucleus, whereas both zymosan and pure β-glucan induced the disappearance of the nuclear protein (Fig. 1*A*). Similar results were observed in macrophages (Fig. 1*B*).

Further experiments showed that the effect of zymosan was elicited by concentrations as low as 0.5 mg/ml (Fig. 1*C*), occurred as soon as 30 min after addition of zymosan (Fig. 1*D*), and lasted for up to 7 h (Fig. 1*E*). Because these findings might point to proteolysis as the main mechanism explaining the disappearance of CHOP from nuclear extracts, the effect of cycloheximide and the proteasome inhibitor MG-132 was assessed. Cycloheximide only partially decreased CHOP expression after 2 h of incubation, and MG-132 did not inhibit CHOP disappearance from the nuclear extracts, thus making it unlikely that translation inhibition and proteasomal degradation could explain the zymosan effect (Fig. 1*F*). Different stimuli were used to analyze the influence of the structure of the β-glucan linkage and the presentation of the stimuli in a particulate state. As shown in the *right panels* of Fig. 1*F*, the insoluble β(1,3)-glucan curdlan and pustulan-containing latex beads induced the disappearance of CHOP from nuclear fractions, whereas the soluble β-glucan laminarin did not induce the disappearance of CHOP. These results suggest that both receptor binding and the particulate state of the stimuli influenced the presence of CHOP in nuclear fractions. Unlike nigeran, all of the β-glucan tested induced *il23a* mRNA. It should be noted that curdlan could only be tested at a lower concentration due to its limited solubility (Fig. 1*G*). Further attempts to disclose possible mechanisms explaining the presence of nuclear CHOP in resting DC focused on signals elicited by components of the culture medium and on the assumption that receptors clustered on lipid rafts might be involved in CHOP expression. Removal of IL-4 did not affect nuclear CHOP expression (data not shown), but elimination of FBS was associated with a reduced expression. However, zymosan also produced the disappearance of CHOP under these conditions (Fig. 2*A*). Unlike atorvastatin,

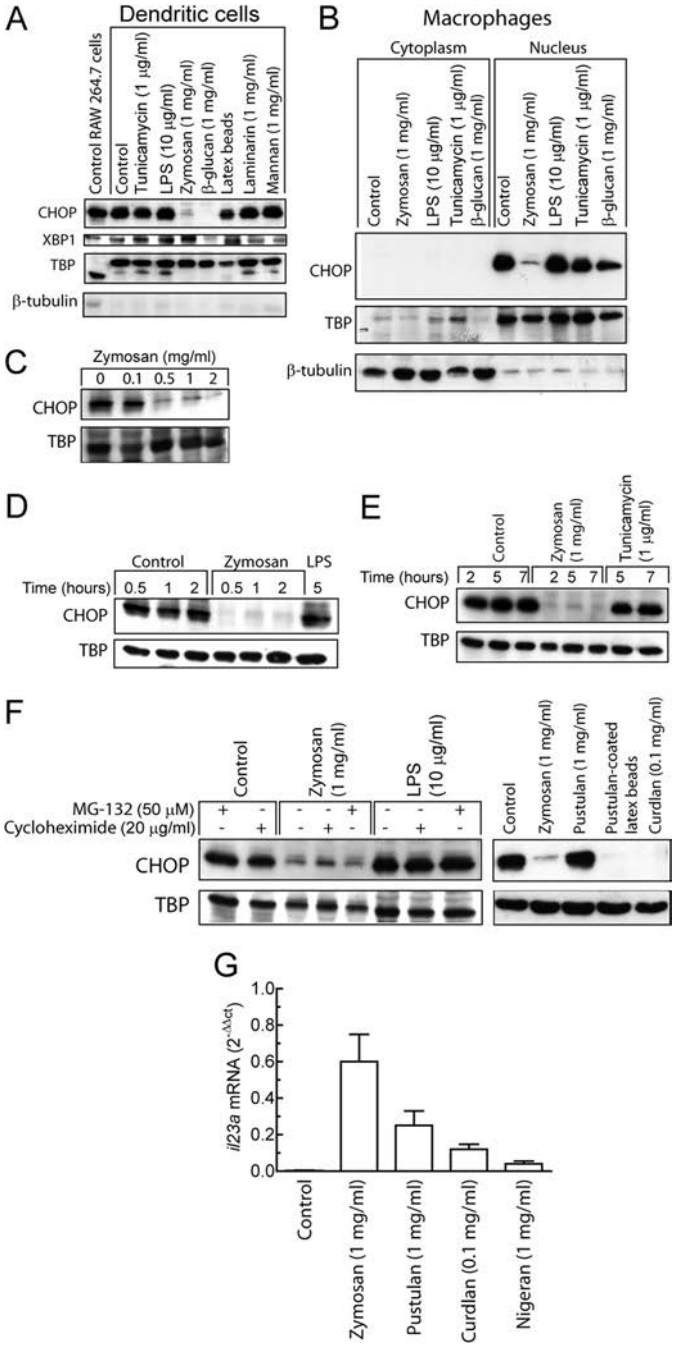

FIGURE 1. **Effect of the incubation of DC with different stimuli on the nuclear expression of CHOP protein.** *A*, DC were incubated for 2 h with different stimuli, and the nuclear extracts were collected for the assay of CHOP and XBP1 protein. TBP and β-tubulin were used as a load control for nuclear and cytoplasmic proteins, respectively. RAW267.7 cells, which constitutively express CHOP as a result of Abelson leukemia virus infection, were used as a reference. This explains the different migration of TBP in this lane. *B*, a representative experiment in human macrophages is shown. *C*, effect of different concentrations of zymosan on nuclear CHOP expression. *D* and *E*, time-dependent disappearance of nuclear CHOP in response to 1 mg/ml zymosan. *F*, effect of the protein synthesis inhibitor cycloheximide and the proteasome inhibitor MG-132 on CHOP protein expression. *Right panel* shows the effect of β-glucans showing distinct structures of linkage on CHOP disappearance. *G*, induction of *il23a* mRNA in DC stimulated for 4 h with glucans with different structures of linkage is shown. Results represent mean ± S.E. of six experiments.

attempts to disrupt lipid rafts with methyl-β-cyclodextrin produced the disappearance of CHOP from nuclear extracts (Fig. 2*B*). Together, these results suggest that signals elicited by serum and involving lipid rafts might be involved in the presence of CHOP in the nuclei of DC.

To address whether shuttling between the nucleus and cytoplasm might explain the disappearance of CHOP from nuclear fractions, laser-scanning confocal fluorescence microscopy was carried out. As shown in Fig. 2*C*, zymosan treatment induced the displacement of CHOP from nuclear and perinuclear areas into the periphery of phagocytosed particles, thus suggesting that shuttling into phagolysosomes could explain its disappearance from the nuclei. Because zymosan phagocytosis does not impede the detection of CHOP by immunofluorescence microscopy and we were unable to detect CHOP in the cytoplasm in Western blots, this can be explained by its retention in vacuoles, post-translational modifications, and/or partial lysosomal degradation that modify its molecular mass and its proper identification by Western blot. Leptomycin B, an inhibitor of nuclear export signal-dependent protein translocation, was used to further address the mechanism of CHOP translocation. Although this treatment produced morphological changes in the DC, it did not influence significantly the subcellular distribution of CHOP either in Western blots (Fig. 2*D*) or in immunofluorescence microscopy (Fig. 2*C*). A way of addressing the mechanism of CHOP induction is assaying the phosphorylation state of eIF2α. As shown in Fig. 2*E*, zymosan induced a slight phosphorylation of eIF2α, whereas tunicamycin, a nucleoside antibiotic that induces the UPR by blocking *N*-linked glycosylation of proteins, produced a marked effect, thus agreeing with the notion that zymosan has a limited effect on the eIF2α cascade. To survey another branch of the UPR, the cleavage of ATF6 was assayed. Stimulation with zymosan for 1 h induced ATF6 cleaving to a very low extent and a clear retardation of full-length ATF6 (Fig. 2*F*), most likely consistent with the glycosylation of the protein before cleavage by site-1 proteases (18). The retarded migration of ATF6 was less clear at 4 h, thus suggesting new synthesis of full-length protein after zymosan phagocytosis. Because cleavage of ATF6 is difficult to detect and the measure of its binding to specific sequences has been used to overcome this difficulty *in vitro*, we assayed the binding of ATF6 to the CHOP-C/EBP, CRE, and ATF2 sites of the *il23a* promoter. No detectable binding was observed in response to both LPS and zymosan (data not shown), thus suggesting that this branch of the UPR is not involved in the transcriptional regulation of *il23a* expression. Given that zymosan is composed of an outer layer of mannoproteins and an inner layer of β-glucans that is accessible on budding yeasts (19) and to extend the significance of the findings to fungal infection, we assessed the effect of latex beads covalently coated with either laminarin or mannan and compared their effects with those produced by *Candida*. As shown in Fig. 3*A*, laminarin coating converted latex beads into a stimulus able to induce the disappearance of CHOP from nuclear fractions. Incubation of DC with heat-inactivated *Candida* (Fig. 3*A*, *right panels*) or with the particulate α-glucan nigeran (Fig. 2*D*) did not induce the disappearance of nuclear CHOP, whereas hypha-forming *Candida* did so (Fig. 3, *A* and *B*). These data indicate that particulate β-glucans induce the disappearance of CHOP from nuclear fractions and its association with phagocytic vesicles in the cytoplasm. This may also occur during fungal hypha formation

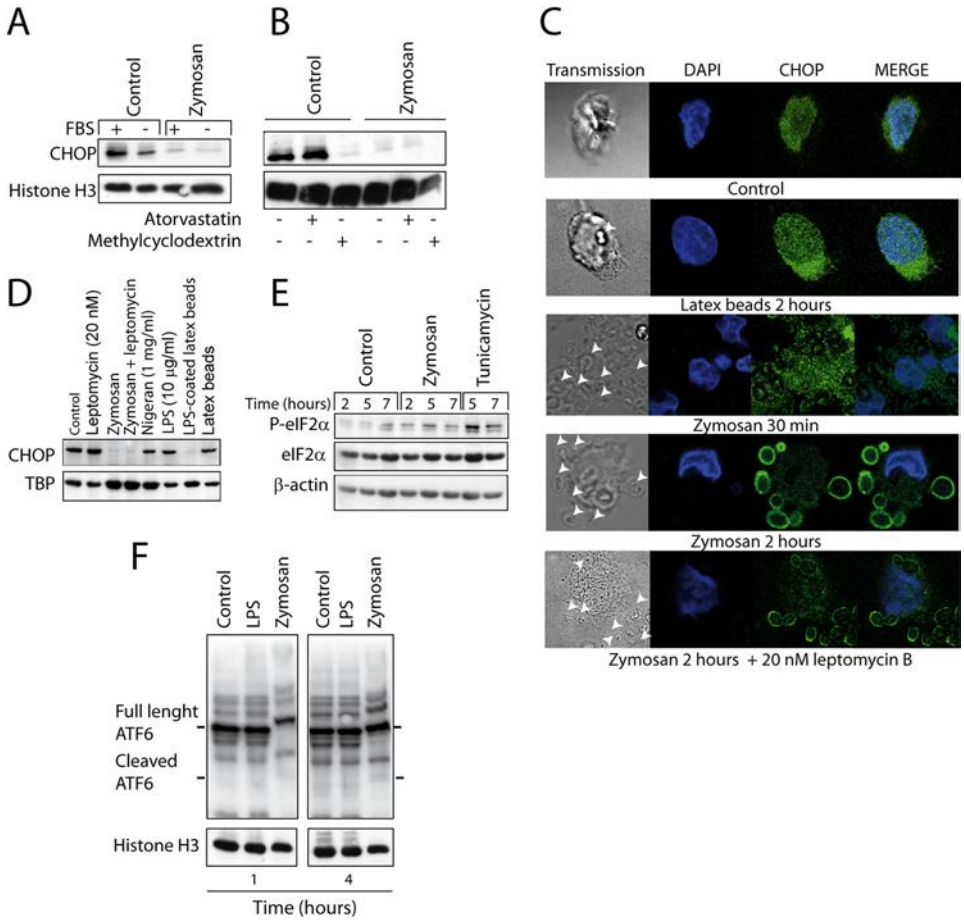

FIGURE 2. **Effect of different treatments on CHOP expression and effect of zymosan and tunicamycin on eIF2α phosphorylation and ATF6 cleavage.** *A*, DC were incubated for 4 days with GM-CSF and IL-4 in the presence of FBS. At the end of this period, the medium was removed and substituted for new medium with or without FBS for 24 h, before stimulation with zymosan for 1 h. CHOP protein was assayed in the nuclear extracts. *B*, DC differentiated in the presence of FBS were incubated for 1 h with 10 mM methyl-β-cyclodextrin or with 10 μM atorvastatin for 24 h and then used for the assay of nuclear CHOP protein. *C*, DC were adhered to polylysine-coated glass coverslips for 12 h and then stimulated for the times indicated with latex beads and zymosan particles in the presence and absence of 20 nM leptomycin B, and processed as described under "Experimental Procedures." Photomicrographs were obtained by laser-scanning confocal fluorescence microscopy. *Arrowheads* indicate the presence of particles in the transmission photomicrographs. *D*, effect of leptomycin, nigeran, and LPS-coated latex beads on nuclear CHOP expression is shown. *E*, DC were treated for the times indicated with 1 mg/ml zymosan or 1 μM tunicamycin, and cell lysates were collected at the times indicated for the assay of eIF2α phosphorylation. *F*, DC treated with 10 μg/ml LPS and 1 mg/ml zymosan were stimulated for the times indicated to address the cleavage of ATF6. Results are representative of at least three independent experiments. *P* indicates phosphate.

and when LPS is presented in a particulate state (Fig. 2*D*). These findings extend previous reports associating TLR3/4 signaling with suppression of the ATF4/CHOP branch of the UPR (20, 21).

Zymosan Is a Weak Activator of XBP1 Splicing—The IRE1α/XBP1 branch of the UPR is independent of the PERK/eIF2α/ATF4 branch, may exert a protective effect on the proapoptotic effect of CHOP, and cooperates with TLR in the innate immune response (22). In addition, it has been described that an increased expression of the spliced form of *XBP1* mRNA coincided with IL-23 production (9). Zymosan induced a time-dependent splicing of *XBP1* as judged from the appearance of both the spliced (*sXBP1*) and hybrid forms of *XBP1* (*hXBP1*) 1 h after zymosan addition, with a peak at 3–5 h and their disappearance at 24 h. Tunicamycin induced a more intense response that could be observed up to 24 h (Fig. 4*A*). This effect was observed at a concentration of zymosan as low as 0.1 mg/ml and was also produced by β-glucan particles but not by LPS, mannan, and laminarin (Fig. 4, *B* and *C*). The true nature of the heteroduplex band in agarose electrophoresis was confirmed by carrying out a new PCR taking as a template the *hXBP1* and *sXBP1* bands. As shown in the *inset* in Fig. 4*A*, the *hXBP1* band yielded three bands, whereas the spliced band only generated one band. In keeping with the dependence of *XBP1* splicing on IRE1α endonuclease activity, the IRE1α inhibitor MKC8866 completely blocked the effect of both zymosan and tunicamycin (Fig. 4*D*). Protein phosphatase type 2A (PP2A) regulates two branches of the UPR. It dephosphorylates IRE1α (23) and prevents endonucleolytic mRNA decay (24). In addition, it dephosphorylates the eIF2B ϵ-subunit and makes it resistant to the phosphorylated form of eIF2α (21). Because PP2A can be activated by 1,9-dideoxyforskolin (ddF) (25), we addressed its effect on *XBP1* splicing. ddF inhibited the splicing of *XBP1* and the induction of CHOP mRNA produced by tunicamycin but not the effect of zymosan (Fig. 5, *A–D*). Further assessment of the modulation of CHOP protein expression by phosphorylation/dephosphorylation reactions was carried out with the serine/threonine phosphatase inhibitor sodium fluoride and the protein-tyrosine phosphatase inhibitor peroxovanadate. As shown in Fig. 5*E*, sodium fluoride did not influence the presence of

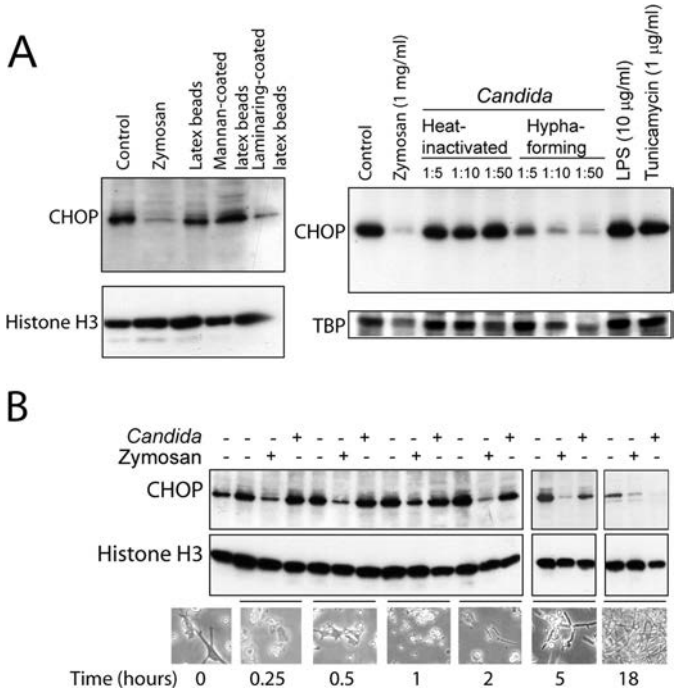

FIGURE 3. **Effect of *Candida* on nuclear CHOP expression.** *A*, DC were stimulated for 2 h with the indicated stimuli and with either heat-inactivated or hypha-forming *Candida* at different DC:*Candida* ratios and then used for the assay of nuclear CHOP protein. *B*, time course experiment showing the formation of hyphae and CHOP disappearance from nuclear fractions of DC after incubation with *Candida* at a ratio of 1:5 DC/*Candida*.

CHOP in nuclear fractions. In contrast, incubation of resting DC with sodium peroxovanadate did induce the disappearance of CHOP protein, thus agreeing with the reported involvement of protein tyrosine phosphorylation reactions in CHOP degradation (26).

Effect of the Pharmacological Modulation of the UPR on Cytokine Production—Taking into account the reports on the involvement of CHOP and XBP1 on *il23a trans*-activation, we studied the effect of inhibitors of the endonuclease activity of IRE1α and pharmacological modulators of sirtuin activity, because SIRT1 activity is strongly enhanced during zymosan phagocytosis (4) and SIRT1 interacts with eIF2α to regulate the cellular stress response (27). As shown in Fig. 6*A*, MKC3946 and MKC8866 inhibited *XBP1* splicing without affecting significantly or even slightly enhancing *chop* mRNA expression, thus suggesting that the PERK/eIF2α/ATF4/CHOP route may be activated by inhibition of *XBP1* splicing (14). The expression of *il23a* and *ptgs2*, which usually show a parallel sensitivity to transcriptional regulators, did not show any significant change in the presence of these compounds. Pharmacological modulation of sirtuin activity by the SIRT1 inhibitor EX-527 and the SIRT1 activator SRT1720 did not modify CHOP expression nor *XBP1* splicing significantly, but an inhibition of *il23a* and *ptgs2* expression was observed by SRT1720 in response to zymosan (Fig. 6*B*).

Transcription Factor Binding to the il23a Promoter—There are several binding sites potentially involved in the transcriptional regulation of *il23a*, as disclosed by the bioinformatics analysis of the promoter with the TRANSFAC database (Fig. 7*A*). In keeping with the disappearance of CHOP protein from

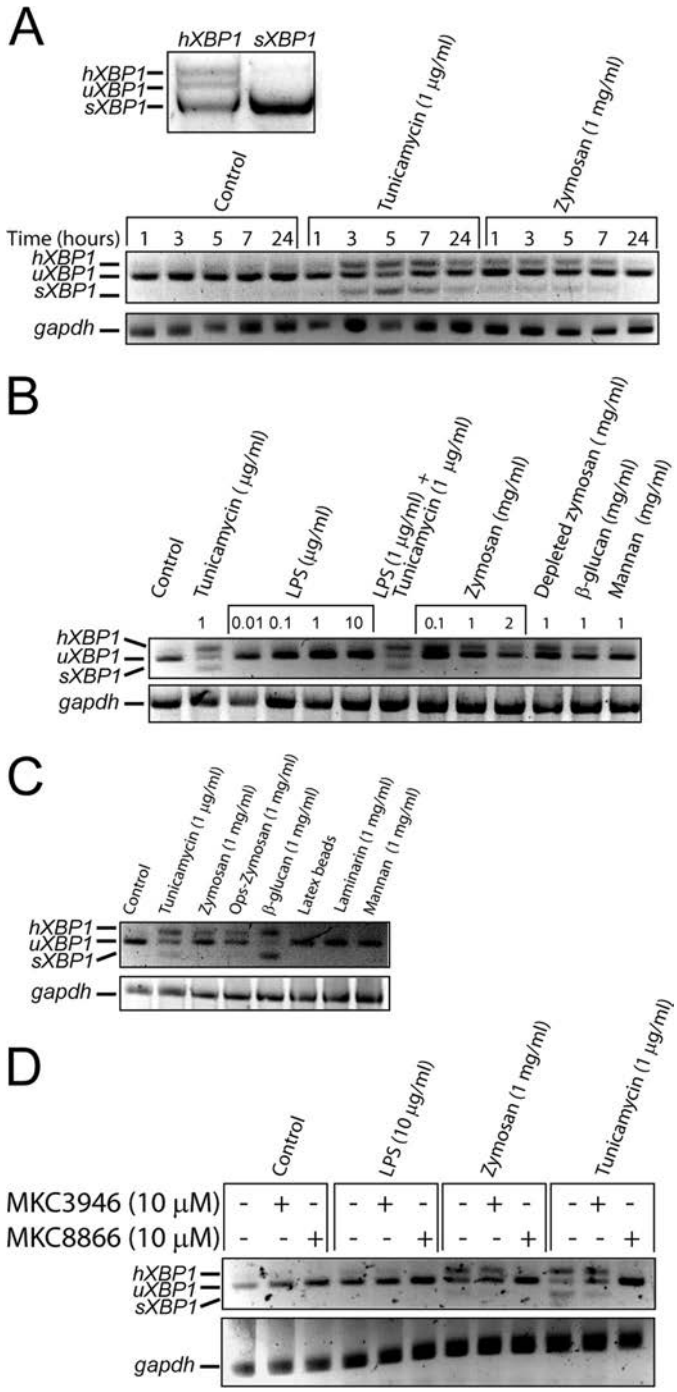

FIGURE 4. **Effect of different stimuli on the splicing of *XBP1*.** *A*, time dependence of *XBP1* splicing in response to tunicamycin and zymosan. *B* and *C*, assay of the effect of different concentrations of stimuli on *XBP1* splicing at a fixed time of 5 h. *D*, effect of the endonuclease domain inhibitors of IRE1α, MKC3946, and MKC8866 on *XBP1* splicing in DC treated for 5 h with different stimuli. *hXBP1* indicates hybrid *XBP1*; *uXBP1* indicates unspliced *XBP1*; *sXBP1* indicates spliced *XBP1*. The *inset* in *A* shows the result of a PCR taking as a template the *hXBP1* and the *sXBP1* bands of DC treated for 5 h with tunicamycin to disclose the presence of *sXBP1* and *uXBP1* in the *hXBP1* band.

the nuclear extracts, zymosan induced a diminution of the binding of CHOP to both CHOP-C/EBP sites (Fig. 7*B*). Consistent with their belonging to the same family of transcription factors, LPS increased the binding of C/EBPβ to CHOP-C/EBP sites and to the −764 C/EBPβ site, whereas zymosan failed to do so (Fig. 7*C*). XBP1 binding to the X2-Boxes did not increase

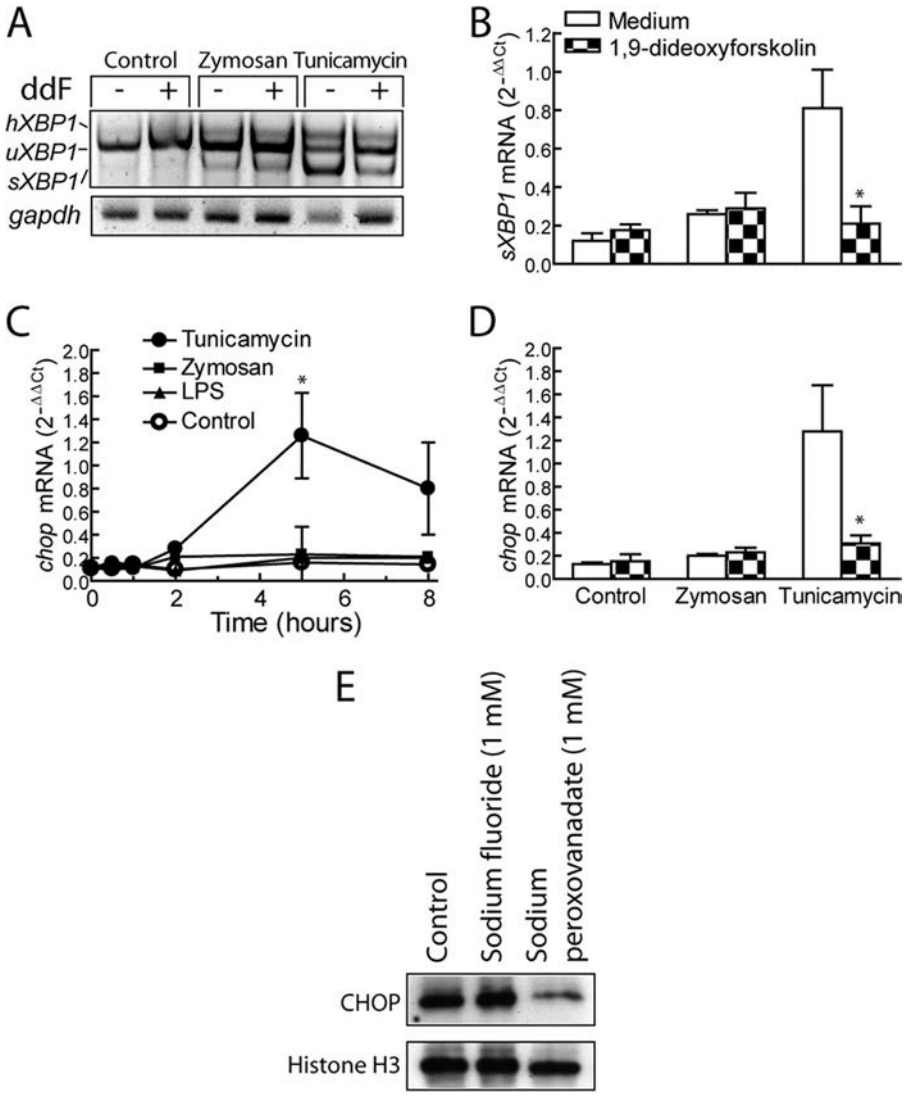

FIGURE 5. **Effect of the pharmacological modulation of PP2A and tyrosine phosphatase activities on the UPR.** *A*, effect of 40 μM ddF on the splicing of *XBP1* elicited by zymosan and tunicamycin at 5 h. *B*, effect of ddF on *XBP1* splicing using a real time RT-PCR assay with a reverse primer overlapping the splice junctions. Zymosan was used at the concentration of 1 mg/ml and tunicamycin at 1 μg/ml. ddF was added 1 h before the stimuli. *C*, effect of zymosan and tunicamycin on *chop* mRNA expression. *D*, effect of ddF on the expression of *chop* mRNA. *E*, effect of the general serine/threonine phosphatase inhibitor sodium fluoride and the protein-tyrosine phosphatase inhibitor peroxovanadate on the expression of CHOP in nuclear fractions of DC incubated for 1 h in the presence of these inhibitors. Results represent mean ± S.E. of three experiments or a representative experiment in *A* and *E*. *, $p < 0.05$.

over resting levels in cells treated with zymosan and LPS 1 h after addition of the stimuli (data not shown), but consistent with the more prominent effect of β-glucan particles on *XBP1* splicing at later times, both commercially depleted zymosan and NaOH-treated zymosan increased more than 2-fold the binding of XBP1 to the X2-Box 5 h after addition of the particles. Tunicamycin produced a higher increase of XBP1 binding and MKC8866 inhibited the binding (Fig. 7*D*). Control experiments with irrelevant Ab did not show increased binding in response to zymosan (Fig. 7, *C* and *D*). CREB binding to the CRE site was detected in resting cells at a similar level to that observed in stimulated cells (Fig. 7*E*), whereas the binding of Ser(P)-133-CREB increased in response to zymosan and to a larger extent with LPS. Notably, zymosan increased robustly the binding of Thr(P)-71–ATF2 to its promoter site 1 h after addition of the stimulus. This was also observed in response to tunicamycin but not to LPS (Fig. 8*A*). In keeping with the notion that ATF2 activation depends on complementary phosphorylations on N-terminal Thr-69 and Thr-71 that depend on PKA, PKC, and MAPK (28–30), modulation of these activities showed a strong inhibition of Thr(P)-71–ATF2 binding by the PKA/mitogen- and stress-activated kinase inhibitor H89, the PKC inhibitor bisindolylmaleimide I, and the MEK inhibitor U0126 but not by the p38 MAPK SB203580 and the JNK inhibitor SP600125 (Fig. 8*A*). To confirm these findings, ATF2 phosphoblots were carried out in nuclear fractions. As shown in Fig. 8*B*, several proteins bands were observed in the area encompassed by the 75 to 52.7-kDa molecular mass protein standards. This is in keeping with the existence of several ATF2 isoforms and the possible occurrence of mobility shifts induced by phosphorylations, all of which contain the Thr-Pro-Thr-Pro sequence. This also agrees with the ChIP results because U0126 but not SP600125 showed a significant inhibition of Thr(P)-71–ATF2 immunoreactivity (Fig. 8*B*). In keeping with the reported

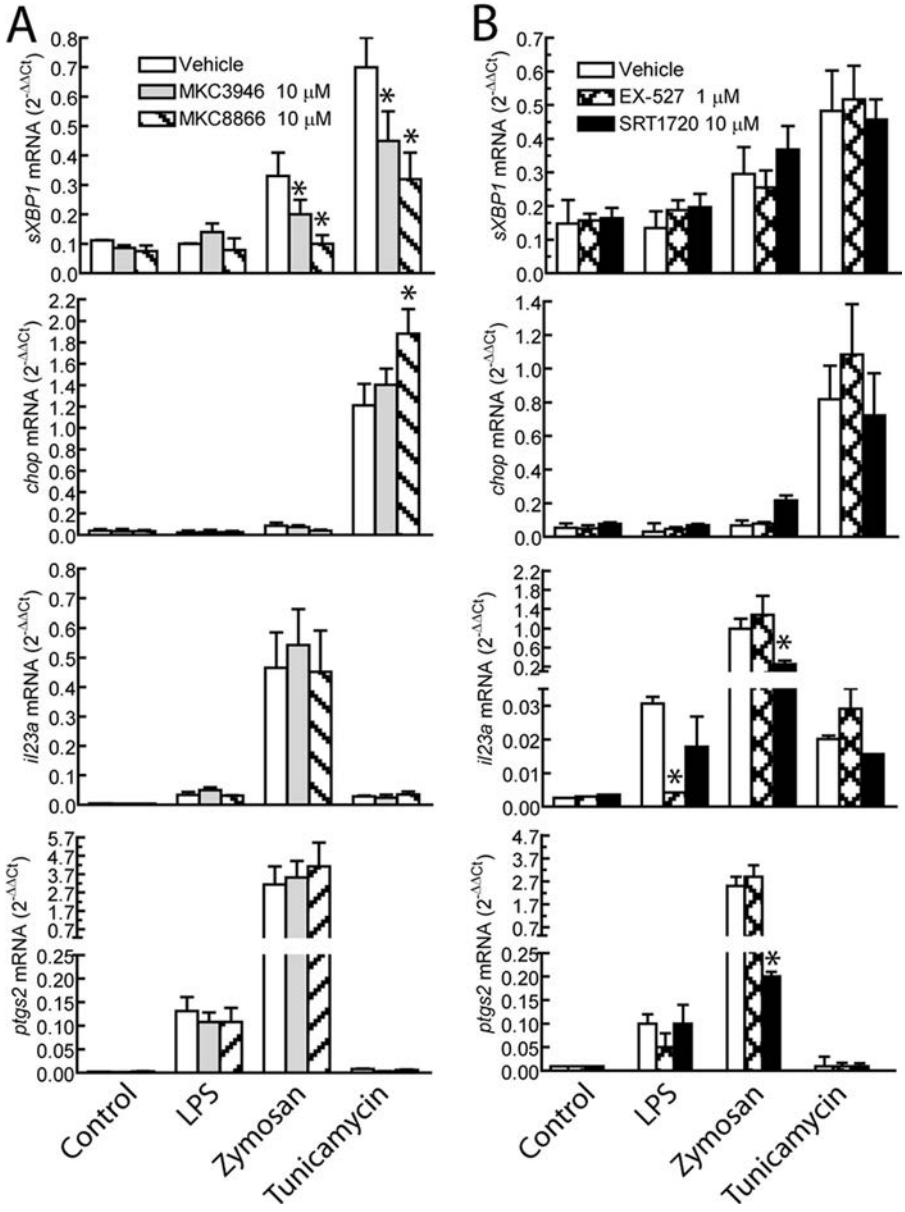

FIGURE 6. **Pharmacological modulation of IRE1α and sirtuin activities.** *A*, effect of the pharmacological modulation of the endonuclease domain activity of IRE1α on the expression of *sXBP1*, *chop*, *il23a*, and *ptgs2* mRNA elicited by LPS, zymosan, and tunicamycin at the usual concentrations. *B*, effect of the pharmacological modulation of sirtuin by the SIRT1 inhibitor EX-527 and the SIRT1 activator SRT1720. DC were incubated for 30 min with vehicle or the indicated drugs and then treated for 4 h with the different stimuli. Results represent mean ± S.E. of 5- 7 experiments. *, $p < 0.05$ as compared with vehicle-treated cells.

dependence of Thr-69 phosphorylation on the attendant phosphorylation on Thr-71, the MEK inhibitor diminished Thr(P)-69-ATF binding 1 h after the addition of zymosan, whereas no binding could be detected at 4 h. In contrast, the JNK inhibitor did not inhibit the binding at any time (Fig. 8*C*). The occurrence of massive binding of ATF2 to the ATF2 site in response to zymosan was also observed with anti-ATF2 Ab (Fig. 8*D*), thus suggesting that under resting conditions there is no binding to the promoter and that this depends on its phosphorylation state. Consistent with the lack of effect of JNK inhibition, binding of c-Jun to the ATF2 site was not detected in ChIP assays (data not shown). When the effect of these inhibitors was addressed on *il23a* expression, unlike the JNK inhibitor, the p38 MAPK inhibitor, the PKC inhibitor, and H89 significantly decreased *il23a* mRNA (Fig. 8*E*). In contrast to the consistent inhibition of Thr-71–ATF2 binding by the MEK inhibitor, we only observed inhibition of *il23a* mRNA expression in three out of six independent experiments that are shown separately in Fig. 8*F*, thus suggesting that there may be alternative mechanisms of transcriptional activation and/or phosphorylation that can bypass the MEK-dependent step. In contrast to the results reported in transfected RAW264.7 (5), binding of ATF2 to the TRE-like X2-Box at −231 was detected to a very low extent, and it did not reach statistical significance (data not shown). Because tunicamycin induced binding of Thr(P)-71–ATF2 to the *il23a* promoter and it has been reported that it enhances the effect of LPS on IL-23 production (8), we addressed the effect of the combination of both stimuli on *il23a* expression. As shown

in Fig. 8*G*, a synergistic induction of *il23a* mRNA was observed, although it did not reach the levels detected with zymosan. Because leucine zipper-containing transcription factors can recognize DNA-binding sites exhibiting similar sequences, we looked at the binding of ATF4 and irrelevant Ab to the ATF2 site. Whereas the irrelevant Ab did not show any significant changes upon zymosan treatment, the binding of ATF4 was enhanced in response to zymosan, LPS, and tunicamycin but to

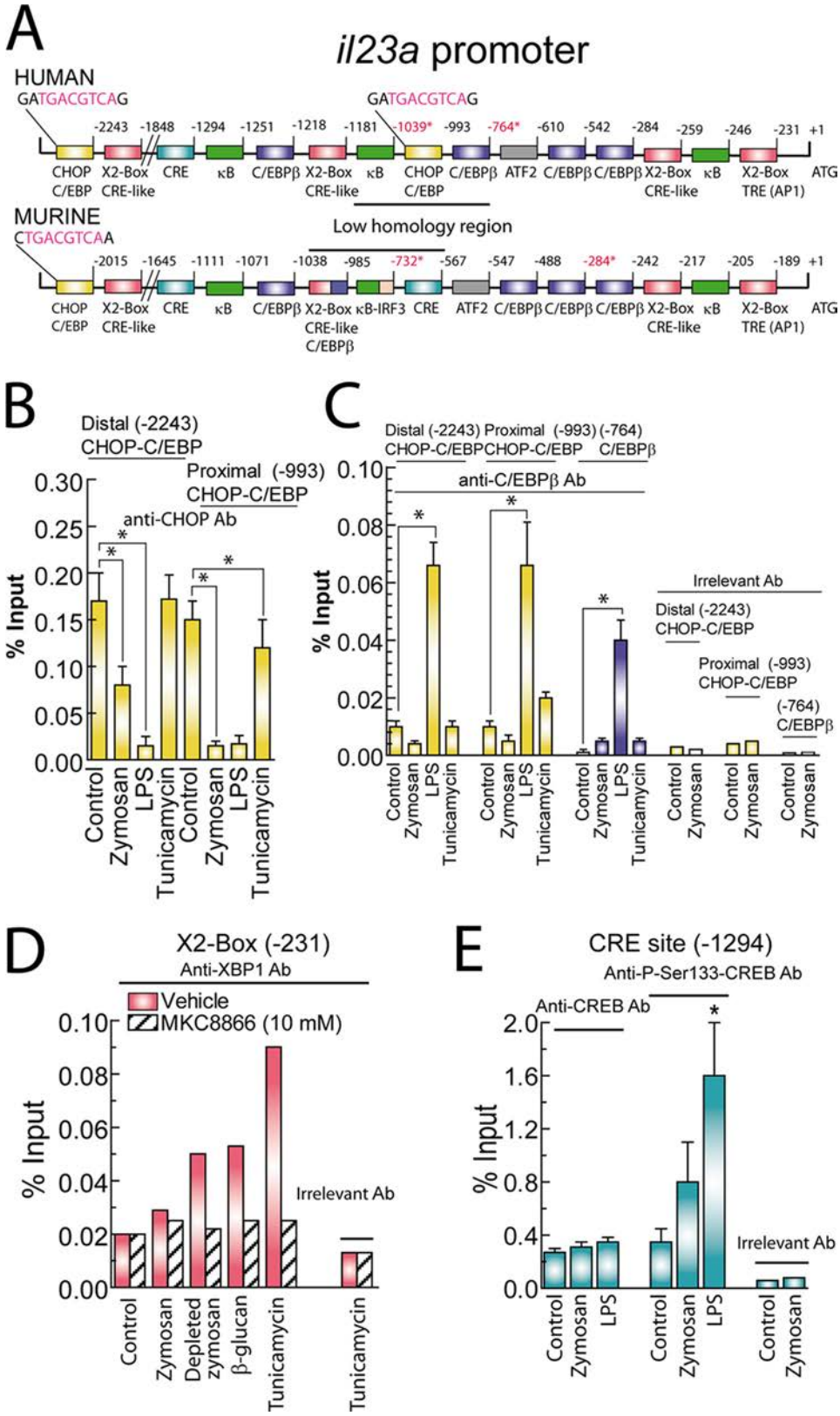

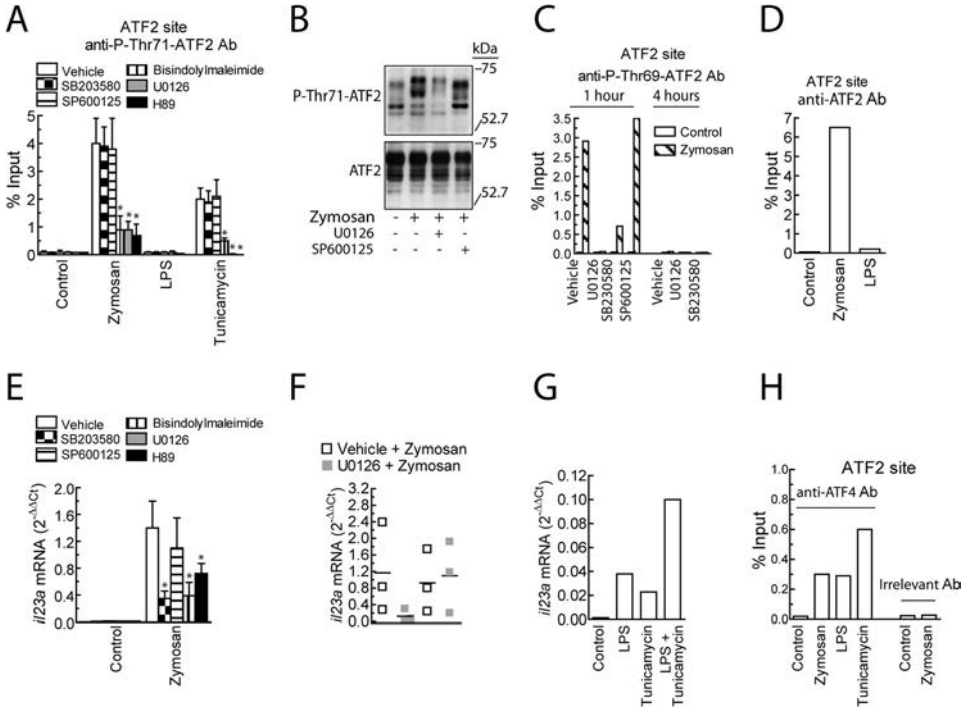

FIGURE 8. **ATF2 binding and *il23a* expression.** *A*, binding of Thr(P)-71–ATF2 to the ATF2 site in the presence and absence of pharmacological inhibitors 1 h after addition of the stimuli. *B*, assay of ATF2 proteins in nuclear fractions of DC stimulated with zymosan for 1 h in the presence and absence of U0126 and SP600125. *C*, binding of Thr(P)-69–ATF2 to the ATF2 site was conducted at 1 and 4 h after zymosan challenge in the presence and absence of U0126, SB203580, and SP600125. This is a typical experiment showing the consistent lack of effect of the JNK inhibitor and the strong effect of MEK inhibitors on Thr(P)-69–ATF2. *D*, ATF2 binding was confirmed by using anti-ATF2 Ab. *E* and *F*, effect of pharmacological inhibitors on *il23a* mRNA expression in response to zymosan. The p38 MAPK inhibitor SB203580, the MEK inhibitor U0126, and the PKA/mitogen- and stress-activated kinase inhibitor H89 were used at 10 μM. The JNK inhibitor SP600125 was used at a concentration of 25 μM. The PKC inhibitor bisindolylmaleimide I was used at a concentration of 0.3 μM. The result of individual experiments in DC stimulated with zymosan in the presence and absence of U0126 is broken down in *E* to disclose that the treatment was effective in three out of six experiments. *G*, effect of LPS, tunicamycin, and combinations thereof on the expression of *il23a* mRNA. *H*, binding of ATF4 and irrelevant control Ab to the ATF2 site. Results represent mean values of two experiments in duplicate. Results represent mean ± S.E. of five experiments in *A* and *D* and mean values of two experiments with a similar trend in *B*, *C*, *F*, and *G*. *, $p < 0.05$ as compared with vehicle-treated cells.

a lower extent than Thr(P)-71–ATF2 binding (Fig. 8*H*), thus suggesting that both transcription factors can bind this site. The variable effect of MEK inhibition on *il23a* expression was further addressed in two experiments where the inhibition of both MEK activity and Thr(P)-71–ATF2 binding by U0126 was confirmed, although *il23a* expression and ATF4 binding were not reduced (Fig. 9, *A–D*). Further analysis of the Thr-69–ATF2 phosphorylation was carried out by assessing the effect of bisindolylmaleimide I and H89. As shown in Fig. 9*E*, both compounds inhibited Thr(P)-69–ATF2 binding to the ATF2 site. Bisindolylmaleimide showed a slight effect on p38 MAPK phosphorylation, but these compounds did not show any effect on ERK phosphorylation (Fig. 9*F*), thus suggesting that PKC may exert an effect upstream of p38 MAPK and that the effect of H89 cannot be explained through an effect on ERK. Further evidence of the involvement of ATF2 on *il23a* expression was carried out by knocking down experiments using nucleofection of siRNA. As shown in Fig. 9*G*, knocking down *atf2* mRNA reduced significantly its expression as well as *il23a* mRNA, whereas *il12/23b* and *il10* mRNA were not affected. Altogether, these data suggest that zymosan has a strong ability to enhance Thr(P)-71-Thr(P)-69–ATF2 binding at the ATF2 site and that ATF2 can be the transcription factor that cooperates preferentially with Rel family proteins to regulate *il23a* transcription. Because inhibition of ATF2 binding associates with the reduction of *il23a* mRNA expression by PKC, PKA/mitogen- and stress-activated kinase, p38 MAPK, and in some cases MEK inhibitors, a functional connection between these events is likely.

DISCUSSION

The purpose of this study has been the analysis of the mechanism of transcriptional regulation of *il23a* expression taking

FIGURE 7. **Binding sites for transcription factors in the *il23a* promoter.** *A*, structure of the *il23a* human and murine promoters showing the most relevant binding sites for transcription factors identified using the TRANSFAC database. Sites are *numbered* taking into account the initial translated methionine. The *red letters* in the CHOP-C/EBP sites indicate the CRE consensus sequence enclosed into the CHOP consensus. There is a region of low homology in both promoters that is marked by a *line*; however, these areas contain binding sites showing analogy and high score values for transcription factor binding in both species. These sites are marked in *red* and with an *asterisk*. *B* and *C*, effect of different stimuli on the binding of CHOP and C/EBPβ to C/EBPβ sites using ChIP assays. Irrelevant Ab were used to show the specificity of transcription factor binding. *D*, effect of commercially available depleted zymosan without TLR2 stimulating activity, β-glucan obtained by NaOH treatment of zymosan, and tunicamycin on the binding of XBP1 to the proximal X2-Box site and inhibition by 10 μM MKC8866. The experiment was conducted in DC collected 5 h after addition of the stimuli, consistent with the occurrence of optimal *XBP1* splicing at this time. *Numbers in parentheses* indicate the position of the sites according to *A*. *E*, binding of CREB and P-Ser133-CREB to the CRE site. DC were stimulated with 1 mg/ml zymosan, 1 μg/ml tunicamycin, and 10 μg/ml LPS for 1 h, unless otherwise indicated, before collecting the samples for ChIP assays. The results represent mean ± S.E. of 3–5 experiments in *B–D*, and a representative experiment in *D*. *, $p < 0.05$.

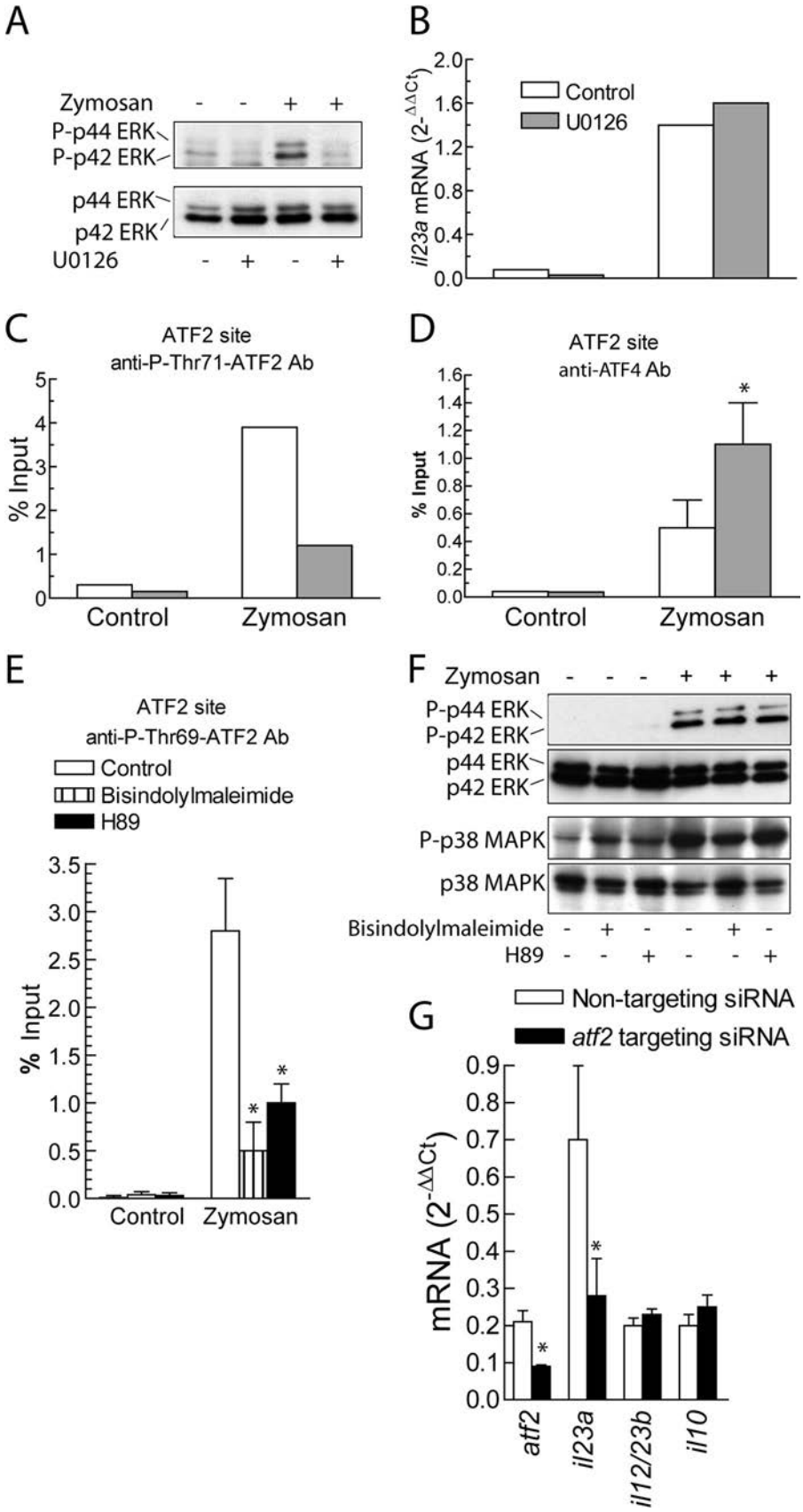
A
Zymosan - - + +
P-p44 ERK
P-p42 ERK
p44 ERK
p42 ERK
U0126 - + - +
B
Control
U0126
il23a mRNA (2-ΔΔCt)
C
ATF2 site
anti-P-Thr71-ATF2 Ab
% Input
Control
Zymosan
D
ATF2 site
anti-ATF4 Ab
% Input
Control
Zymosan
E
ATF2 site
anti-P-Thr69-ATF2 Ab
Control
Bisindolylmaleimide
H89
% Input
Control
Zymosan
F
Zymosan - - - + + +
P-p44 ERK
P-p42 ERK
p44 ERK
p42 ERK
P-p38 MAPK
p38 MAPK
Bisindolylmaleimide - + - - + -
H89 - - + - - +
G
Non-targeting siRNA
atf2 targeting siRNA
mRNA (2-ΔΔCt)
atf2
il23a
il12/23b
il10

into account the available data regarding the cooperation of different transcription factors and the selectivity of the fungal surrogate zymosan to induce IL-23. In addition to deciphering the network of transcription factors involved, our data have shown unexpected data regarding ERS/UPR and phagocytosis of fungal particles. The first hypothesis we considered stemmed from the reported roles of CHOP and XBP1 in combination with NF-κB proteins in the *trans*-activation of *il23a* and the close association of IL-23 and the UPR in ankylosing spondylitis. Unexpectedly, DC in the resting state showed the expression of CHOP protein in nuclear fractions at levels that made it difficult to assess net increases upon treatment with tunicamycin, even though this agent increased CHOP mRNA and induced the phosphorylation of eIF2α, consistent with the activation of the PERK/eIF2α/ATF4/CHOP cascade. In addition, zymosan produced the disappearance of CHOP from nuclear fractions in a time- and dose-dependent manner. Approaches directed to assess the mechanism of nuclear CHOP protein disappearance showed that it was triggered by particulate stimuli and was rather insensitive to cycloheximide and MG-132, thus making it unlikely a straightforward association with proteasomal degradation. This agrees with reports showing that CHOP is degraded with a half-life of 4 h in the presence of cycloheximide (31) and that it is not degraded in the proteasome in all cell types (32). In keeping with the reported ability of CHOP to shuttle between nucleus and cytoplasm (33), we next addressed the occurrence of cytoplasmic translocation. Our data showed a close association of CHOP with what most likely represent phagocytic vesicles, even in the presence of leptomycin B, which indicates that CHOP shuttling does not involve a mechanism of protein export dependent on nuclear export sequences. Unlike atorvastatin, which affects receptor clustering via lipid raft modulation, attempts to disrupt lipid rafts with methyl-β-cyclodextrin produced the disappearance of CHOP from nuclear extracts. This can be explained by the possible usage of stored lipids even when the *de novo* cholesterol synthesis is inhibited by atorvastatin, whereas methyl-β-cyclodextrin might mimic the effect of β-glucans because it is composed of β(1,4)-glucans that may be phagocytosed by receptor-dependent mechanisms. Because the expression of CHOP depends on phosphorylation reactions, we addressed the effect of phosphatase inhibitors, and results showed that displacement of the protein tyrosine phosphorylation balance by inhibition of protein-tyrosine phosphatases induced the disappearance of CHOP from the nuclear fractions. This finding agrees with the critical role of CHOP Tyr-22 in the constitutive degradation of CHOP (26) and is reminiscent of the report by Underhill and co-workers (34) showing that intracellular signaling by β-glucan complexes depends on the exclusion of inhibitory phosphatases from the "phagocytic synapse." The relevance of these findings to fungal infection was confirmed by showing that the disappearance of CHOP proteins was produced by *Candida* in parallel with the formation of hyphae and the attendant exposure of β-glucans on budding yeasts. Since it has recently been disclosed that a unique close-chain chemical structure of hyphal β-glucans induce a robust production of proinflammatory responses (35), it is possible that the presence of cyclical β-glucans might explain the different effects of yeast and hyphal *Candida* on nuclear CHOP. These findings might have two relevant consequences. First, fungal phagocytosis seems associated with a mechanism directed to preserve phagocytic cells by countering the proapoptotic effect of CHOP. Second, the disappearance of CHOP from nuclear extracts fits well with the concept of the inhibitory effect of CHOP on transcription. In fact, the role of CHOP as a dominant-negative component of CHOP-C/EBPβ heterodimers and the ensuing enhancement of C/EBPβ-dependent transcription upon CHOP degradation were established since its initial identification (36).

Although LPS did not induce the disappearance of CHOP from nuclear fractions, a decrease of CHOP binding was also observed, which most probably indicates that C/EBPβ activation following TLR4 signaling can counter the inhibitory effect of CHOP on *il23a* promoter binding.

Our findings agree with most recent reports challenging the role of CHOP in IL-23 induction in patients of ankylosing spondylitis (37, 38). XBP1 binding to the proximal X2-Box was observed 5 h after stimulation with pure β-glucans. This finding, although consistent with the activation of IRE1α activity, cannot be straightforwardly considered of relevance for *il23a* induction, because the inhibition of the endonuclease activity of IRE1α by MKC8866 did not influence *il23a* expression.

A remarkable effect of zymosan was a prominent induction of ATF2 binding to an ATF2 site, the functional relevance of which was suggested in a previous study in RAW264.7 cells infected with Theiler's murine encephalomyelitis virus (6). Moreover, a study on RAW264.7 cells co-transfected with ATF2, c-Jun, and the *il23a* promoter constructs and stimulated with LPS showed enhancement of promoter activity, whereas *trans*-activation was not observed when the transfection was carried out with a promoter mutated in the TRE-like X2-Box (5). ATF2 could also be involved in the response to tunicamycin, because tunicamycin enhanced ATF2 binding to the *il23a* promoter, thus suggesting that in addition to the proposed mechanism of action through CHOP activation, tunicamycin could cooperate with LPS-induced κB-dependent transcription to *trans*-activate *il23a* via ATF2. In fact, activation of ATF2 by tunicamycin and the cooperation of ATF2 with ATF4 to induce CHOP transcription under amino acid deprivation have been reported (39). The enhancement of C/EBPβ binding to CHOP-C/EBP and C/EBP sites by LPS can also explain the strong ability of LPS to activate *il12/23b* expression, which is regulated by the combined activation of NF-κB and C/EBPβ (40). The path-

FIGURE 9. **Effect of U0126 on ERK activity and Thr(P)-71–ATF2 and ATF4 binding to the ATF2 site in experiments where MEK activity was inhibited but not the expression of *il23a* mRNA.** *A*, inhibition of p42- and p44-ERK phosphorylation by U0126 assayed with a phosphospecific Ab in DC incubated with either vehicle or 10 μM U0126 for 30 min and then stimulated with zymosan for 30 min. *B*, effect of U0126 on *il23a* mRNA expression. *C*, binding of Thr(P)-71–ATF2 to the ATF2 site in the presence and absence of U0126. *D*, binding of ATF4 in the presence and absence of U0126. *E* and *F*, effect of bisindolylmaleimide and H89 on Thr(P)-69–ATF2 binding and ERK and p38 MAPK phosphorylation. *G*, effect of *atf2* knockdown on *atf2* and cytokine expression in DC stimulated with zymosan. Samples were taken 4 h after zymosan challenge for the mRNA assays and at 1 h for binding assays. Results represent mean values of two experiments in *B* and *C*, and mean ± S.E. of three experiments in *D* and *G*, and four in *E*. *, $p < 0.05$.

ways triggered by zymosan revolve around the β-glucan receptor dectin-1, which, unlike the TLR4/LPS route, activates the tyrosine kinase SYK, phospholipase Cγ2, and the Ca^{2+} and diacylglycerol/PKC routes. Because ATF2 is activated by phosphorylations dependent on PKC and MAPK activities, it seems a likely target of dectin-1 signaling. The correlation between inhibition of Thr(P)-71–ATF2 binding and blunting of *il23a* mRNA expression in response to PKC inhibitors can be explained by the upstream position of this kinase, in particular the PKCδ isoform, in dectin-1-mediated cytokine production (41). Our findings that MEK1/2 inhibition blocks the binding of Thr(P)-71–Thr-69–ATF2 and the p38 MAPK inhibitor blunts both mRNA expression and Thr-69–ATF2 binding, but not Thr(P)-71–ATF2 binding, can be explained by the complex mechanism of regulation of ATF2 activity, which was the first example of complementary phosphorylation of a single substrate by ERK and p38 MAPK. In fact, the Ras/Raf/MEK/ERK route phosphorylates Thr-71, whereas p38 MAPK phosphorylates Thr-69 (28), which is central to *trans*-activating activity. To our surprise, the MEK inhibitor did not block *il23a* mRNA expression in some cases, although it was consistently active in the inhibition of Thr-71–ATF2 binding. A plausible explanation for this contradictory finding could be that the treatment with U0126 was not always effective. However, when mRNA expression, transcription factor binding, and MEK inhibition were assayed in the same set of cells (Fig. 9), we observed that *il23a* mRNA expression could be detected even when MEK activity and binding of Thr(P)-71–ATF2 were significantly inhibited. Another explanation consistent with our findings was provided in a recent study on the MAP3K/MAP2K/MEK6/p38 MAPK/ATF2 cascade, where it was reported that phosphorylation of Thr-71–ATF2 by p38 MAPK preceded Thr-69–ATF2 phosphorylation (42). Because ATF2 activity is associated with the second phosphorylation event, it seems likely that in some cases p38 MAPK might account for both phosphorylations, which agrees with the finding of residual Thr-71 and Thr-69 phosphorylation in the presence of U0126 reported in early studies. This is not completely unexpected in view of the importance of the feedback loops that control MAPK activity and contribute to fine-tune cytokine production (43). Moreover, the hypothesis of a two-step mechanism of phosphorylation of ATF2 by the ERK and p38 MAPK has been complemented by recent studies showing that single phosphorylation at Thr-180 of p38 MAPK is sufficient to switch the kinase to an active state capable of phosphorylating Thr-69–ATF2, whereas doubly phosphorylated Thr-180–Tyr-182–p38 MAPK yields doubly phosphorylated Thr-69–Thr-71–ATF2 (44). This agrees with current views stressing that the main role of phosphotyrosine of MAPKs seems to be in substrate recognition, particularly in determining the specificity of the kinase toward peptide substrates with a Pro + 1 (45), which in fact is a feature of Thr-69 and Thr-71 in ATF2. In addition, monophosphorylated p38 MAPK has been detected in macrophages after LPS treatment (46), which is in keeping with the notion that during activation of MAPKs there is a monophosphorylated intermediate (47) and with the finding that phosphatases can contribute to this by dephosphorylating only one of the two phosphoacceptors. Notably, cross-talk between PKA and

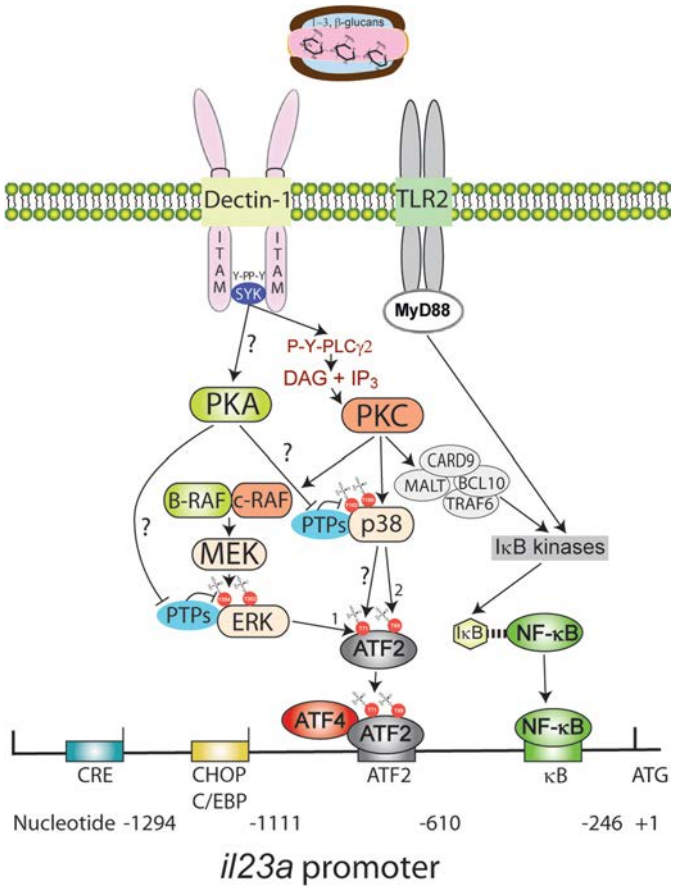

FIGURE 10. **Proposed mechanism of *il23a* induction in response to zymosan.** Binding of fungal patterns activates the proteins of the NF-κB family and a phosphorylation cascade involving at least PKC and MAPK that phosphorylates ATF2 at Thr-69 and Thr-71 and allows the combined action of at least two transcription factors on the *il23a* promoter. Activation of MEK by B-RAF and c-RAF heterodimers depends on upstream kinases. Cross-talk with the MAPK routes can be exerted through protein-protein interaction with tyrosine-specific phosphatases. *DAG*, diacylglycerol; *IP_3*, inositol trisphosphate; *ITAM,* immunoreceptor tyrosine-based activation motif; *PLCγ2*, phospholipase Cγ2; *P-Y*, phosphotyrosine; *PTPs*, tyrosine-specific phosphatases; *SYK*, spleen tyrosine kinase. *Numbers 1* and *2* indicate the most accepted order of events leading to ATF2 Thr-71 and Thr-69 phosphorylation. Possible signaling events not directly addressed in the experiments are indicated with a *question mark*.

MAPK cascades can occur via phosphorylation by PKA of the N-terminal kinase interaction motif of tyrosine-specific phosphatases such as HePTP and PTP-SL (Fig. 10), which inhibits protein-protein interactions with ERK and p38 MAPKs and allows their nuclear translocation (48–51). The difficulty assessing the extent of monophosphorylated intermediates is that most phosphospecific antibodies may recognize MAPKs phosphorylated either individually or dually (47). On this basis, the effect of PKA and PKC on ATF2 phosphorylation may be indirect and exerted at different levels (Fig. 10). Taking into account the two-step distributive (nonprocessive) mechanism of ATF2 phosphorylation (42, 52), it seems likely that ERK activity may be most active to phosphorylate Thr-71, but in the absence of ERK activity, Thr-180–Tyr-182–p38 MAPKs might yield doubly phosphorylated Thr-69–Thr-71–ATF2.

Direct evidence of the involvement of ATF2 has been obtained by showing that knockdown of *atf2* mRNA shows a strong correlation with the inhibition of *il23a* mRNA but not with those of *il12/23b* and *il10*. However, the involvement of an

alternative enhanceosome containing C/EBPβ, CREB, or ATF4 seems also likely under some conditions. In fact, we have observed that zymosan slightly enhances Ser(P)-133-CREB and ATF4 binding to the *il23a* promoter, even in the presence of U0126, although an increased binding of the unphosphorylated protein could not be demonstrated. This agrees with our previous findings showing high levels of CREB in the nuclear extracts of resting DC (15) and with current notions on CREB activation stressing the phosphorylation of the inactive transcription factor already bound to the promoter and a complex interplay of kinases and coactivators (53). Contrary to our initial expectation, we did not observe any effect on JNK inhibition, and in some cases we found an increase of c-Jun binding to the ATF2 site in the presence of the JNK inhibitor SP600125. Although phosphorylation of ATF2 by JNK on threonine residues within the N-terminal activation domain is a hallmark of ATF2 transcriptional responses (54), there may be some explanations for our findings. For instance, sequential phosphorylation by ERK and p38 MAPK has been reported in fibroblasts where JNK is poorly activated by growth factors (28, 55). Another study in JNK1/2$^{-/-}$ double knock-out embryos confirmed the phosphorylation of ATF2 by p38 and ERK, with Ser-90 being the only phosphorylation absolutely dependent on JNK (56). Thr-71 phosphorylation in response to hyperosmotic stress can be carried out by Polo-like kinase 3 in the absence of JNK and p38 MAPK activity in human corneal epithelial cells (57). In other words, it seems possible that Thr-ATF2 phosphorylation can be cell- and/or stimulus-dependent and that the role of JNK1/2 may be more associated with hyperosmosis and cellular stresses, whereas in other systems p38 MAPK and ERK are used preferentially. Another explanation for this finding could be that binding of JNK to ATF2 limits its availability by promoting its degradation (58). The involvement of PKA in *il23a* regulation could be supported by the robust ability of agents that increase the intracellular levels of cAMP to enhance *il23a* expression and the aforementioned effect of H89. In addition, PKA has been associated with the synergistic effect of prostaglandin E_2 on the response to TNFα (7) and LPS (59). However, the actual involvement of prostaglandin E_2 as an autocrine mediator has not been proved unambiguously. For instance, COX inhibition by a high concentration of indomethacin showed a weak inhibitory effect (7). A note of caution regarding the straightforward translation of the results on *il23a* transcription to the overall production of IL-23 arises from the possible influence of concomitant factors such as the parallel production of the IL-12/23 p40 chain and *il23a* mRNA stability (60). In summary, our results have disclosed the presence of CHOP protein in the nuclear extracts of resting DC. Nuclear CHOP undergoes a rapid disappearance upon challenge with β-glucan particles and *Candida* hyphae that rules out a role for this transcription factor in the induction of *il23a* and rather suggests its association with prevention of apoptosis in phagocytosing DC and enhancement of C/EBPβ activity. We have observed remarkable differences in the array of transcription factors activated by β-glucans and LPS, and the most outstanding finding was a strong activation by zymosan of ATF2. The activation of ATF2 upon zymosan challenge seems related to the ability of dectin-1 to activate a phospholipase Cγ2/PKC route with robust effects on downstream MAPK cascades (Fig. 10).

Acknowledgments—Dr. Jesús Pla is thanked for the gift of Candida albicans. Dr. John Patterson is thanked for providing the IRE1α inhibitors MKC3946 and MKC8866. Drs. Carlos R. Vázquez de Aldana and Francisco del Rey are thanked for the gift of nigeran. The staff from Centro de Hemoterapia de Castilla y León is thanked for help with blood cell purification.

REFERENCES

1. Dennehy, K. M., Willment, J. A., Williams, D. L., and Brown, G. D. (2009) Reciprocal regulation of IL-23 and IL-12 following co-activation of Dectin-1 and TLR signaling pathways. *Eur. J. Immunol.* **39,** 1379–1386
2. Huang, H., Ostroff, G. R., Lee, C. K., Wang, J. P., Specht, C. A., and Levitz, S. M. (2009) Distinct patterns of dendritic cell cytokine release stimulated by fungal β-glucans and toll-like receptor agonists. *Infect. Immun.* **77,** 1774–1781
3. Alvarez, Y., Municio, C., Hugo, E., Zhu, J., Alonso, S., Hu, X., Fernández, N., and Sánchez Crespo M. (2011) Notch- and transducin-like enhancer of split (TLE)-dependent histone deacetylation explain interleukin 12 (IL-12) p70 inhibition by zymosan. *J. Biol. Chem.* **286,** 16583–16595
4. Alvarez, Y., Rodríguez, M., Municio, C., Hugo, E., Alonso, S., Ibarrola, N., Fernández, N., and Crespo, M. S. (2012) Sirtuin 1 is a key regulator of the IL-12 p70/IL-23 balance in human dendritic cells. *J. Biol. Chem.* **287,** 35689–35701
5. Liu, W., Ouyang, X., Yang, J., Liu, J., Li, Q., Gu, Y., Fukata, M., Lin, T., He, J. C., Abreu, M., Unkeless, J. C., Mayer, L., and Xiong, H. (2009) AP-1 activated by toll-like receptors regulates expression of IL-23 p19. *J. Biol. Chem.* **284,** 24006–24016
6. Al-Salleeh, F., and Petro, T. M. (2008) Promoter analysis reveals critical roles for SMAD-3 and ATF-2 in expression of IL-23 p19 in macrophages. *J. Immunol.* **181,** 4523–4533
7. Kocieda, V. P., Adhikary, S., Emig, F., Yen, J. H., Toscano, M. G., and Ganea, D. (2012) Prostaglandin E_2-induced IL-23p19 subunit is regulated by cAMP-responsive element-binding protein and C/AATT enhancer-binding protein β in bone marrow-derived dendritic cells. *J. Biol. Chem.* **287,** 36922–36935
8. Goodall, J. C., Wu, C., Zhang, Y., McNeill, L., Ellis, L., Saudek, V., and Gaston, J. S. (2010) Endoplasmic reticulum stress-induced transcription factor, CHOP, is crucial for dendritic cell IL-23 expression. *Proc. Natl. Acad. Sci. U.S.A.* **107,** 17698–17703
9. Wang, Q., Franks, H. A., Lax, S. J., El Refaee, M., Malecka, A., Shah, S., Spendlove, I., Gough, M. J., Seedhouse, C., Madhusudan, S., Patel, P. M., and Jackson, A. M. (2013) The ataxia telangiectasia mutated kinase pathway regulates IL-23 expression by human dendritic cells. *J. Immunol.* **190,** 3246–3255
10. Cláudio, N., Dalet, A., Gatti, E., and Pierre, P. (2013) Mapping the crossroads of immune activation and cellular stress response pathways. *EMBO J.* **32,** 1214–1224
11. Kollnberger, S., Bird, L. A., Roddis, M., Hacquard-Bouder, C., Kubagawa, H., Bodmer, H. C., Breban, M., McMichael, A. J., and Bowness, P. (2004) HLA-B27 heavy chain homodimers are expressed in HLA-B27 transgenic rodent models of spondyloarthritis and are ligands for paired Ig-like receptors. *J. Immunol.* **173,** 1699–1710
12. Ciccia, F., Bombardieri, M., Principato, A., Giardina, A., Tripodo, C., Porcasi, R., Peralta, S., Franco, V., Giardina, E., Craxi, A., Pitzalis, C., and Triolo, G. (2009) Overexpression of interleukin-23, but not interleukin-17, as an immunologic signature of subclinical intestinal inflammation in ankylosing spondylitis. *Arthritis Rheum.* **60,** 955–965
13. Neises, B., and Steglich, W. (1978) Simple method for the esterification of carboxylic acids. *Angew. Chem. Int. Ed.* **17,** 522–524
14. Mimura, N., Fulciniti, M., Gorgun, G., Tai, Y. T., Cirstea, D., Santo, L., Hu, Y., Fabre, C., Minami, J., Ohguchi, H., Kiziltepe, T., Ikeda, H., Kawano, Y., French, M., Blumenthal, M., Tam, V., Kertesz, N. L., Malyankar, U. M., Hokenson, M., Pham, T., Zeng, Q., Patterson, J. B., Richardson, P. G.,

Munshi, N. C., and Anderson, K. C. (2012) Blockade of XBP1 splicing by inhibition of IRE1α is a promising therapeutic option in multiple myeloma. *Blood* **119,** 5772–5781
15. Alvarez, Y., Municio, C., Alonso, S., Sánchez Crespo, M., and Fernández, N. (2009) The induction of IL-10 by zymosan in dendritic cells depends on CREB activation by the coactivators CREB-binding protein and TORC2 and autocrine PGE_2. *J. Immunol.* **183,** 1471–1479
16. Riek, A. E., Oh, J., Sprague, J. E., Timpson, A., de las Fuentes, L., Bernal-Mizrachi, L., Schechtman, K. B., and Bernal-Mizrachi, C. (2012) Vitamin D suppression of endoplasmic reticulum stress promotes an antiatherogenic monocyte/macrophage phenotype in type 2 diabetic patients. *J. Biol. Chem.* **287,** 38482–38494
17. Iwakoshi, N. N., Pypaert, M., and Glimcher, L. H. (2007) The transcription factor XBP-1 is essential for the development and survival of dendritic cells. *J. Exp. Med.* **204,** 2267–2275
18. Hong, M., Luo, S., Baumeister, P., Huang, J. M., Gogia, R. K., Li, M., and Lee, A. S. (2004) Underglycosylation of ATF6 as a novel sensing mechanism for activation of the unfolded protein response. *J. Biol. Chem.* **279,** 11354–11363
19. Clavaud, C., Aimanianda, V., and Latge, J. P. (2009) in *Chemistry, Biochemistry, and Biology of 1–3 β-Glucans and Related Polysaccharides* (Bacic, A., Fincher, G. B., and Stone, B. A., eds) pp. 387–424, Academic Press, New York
20. Woo, C. W., Cui, D., Arellano, J., Dorweiler, B., Harding, H., Fitzgerald, K. A., Ron D., and Tabas, I. (2009) Adaptive suppression of the ATF4-CHOP branch of the unfolded protein response by toll-like receptor signalling. *Nat. Cell Biol.* **11,** 1473–1480
21. Woo, C. W., Kutzler, L., Kimball, S. R., and Tabas, I. (2012) Toll-like receptor activation suppresses ER stress factor CHOP and translation inhibition through activation of eIF2B. *Nat. Cell Biol.* **14,** 192–200
22. Martinon, F., Chen, X., Lee, A. H., and Glimcher, L. H. (2010) TLR activation of the transcription factor XBP1 regulates innate immune responses in macrophages. *Nat. Immunol.* **11,** 411–418
23. Qiu, Y., Mao, T., Zhang, Y., Shao, M., You, J., Ding, Q., Chen, Y., Wu, D., Xie, D., Lin, X., Gao, X., Kaufman, R. J., Li, W., and Liu, Y. (2010) A crucial role for RACK1 in the regulation of glucose-stimulated IRE1α activation in pancreatic β-cells. *Sci. Signal.* **3,** ra7
24. Han, D., Lerner, A. G., Vande Walle, L., Upton, J. P., Xu, W., Hagen, A., Backes, B. J., Oakes, S. A., and Papa, F. R. (2009) IRE1α kinase activation modes control alternate endoribonuclease outputs to determine divergent cell fates. *Cell* **138,** 562–575
25. Neviani, P., Santhanam, R., Trotta, R., Notari, M., Blaser, B. W., Liu, S., Mao, H., Chang, J. S., Galietta, A., Uttam, A., Roy, D. C., Valtieri, M., Bruner-Klisovic, R., Caligiuri, M. A., Bloomfield, C. D., Marcucci, G., and Perrotti, D. (2005) The tumor suppressor PP2A is functionally inactivated in blast crisis CML through the inhibitory activity of the BCR/ABL regulated SET protein. *Cancer Cell* **8,** 355–368
26. Ohoka, N., Hattori, T., Kitagawa, M., Onozaki, K., and Hayashi, H. (2007) Critical and functional regulation of CHOP (C/EBP homologous protein) through the N-terminal portion. *J. Biol. Chem.* **282,** 35687–38694
27. Ghosh, H. S., Reizis, B., and Robbins, P. D. (2011) SIRT1 associates with eIF2α and regulates the cellular stress response. *Sci. Rep.* **1,** 10.1038/srep00150
28. Ouwens, D. M., de Ruiter, N. D., van der Zon, G. C., Carter, A. P., Schouten, J., van der Burgt, C., Kooistra, K., Bos, J. L., Maassen, J. A., and van Dam, H. (2002) Growth factors can activate ATF2 via a two-step mechanism: phosphorylation of Thr-71 through the Ras-MEK-ERK pathway and of Thr-69 through RalGDS-Src-p38. *EMBO J.* **21,** 3782–3793
29. Chen, D., Reierstad, S., Lin, Z., Lu, M., Brooks, C., Li, N., Innes, J., and Bulun, S. E. (2007) Prostaglandin E_2 induces breast cancer related aromatase promoters via activation of p38 and c-Jun NH_2-terminal kinase in adipose fibroblasts. *Cancer Res.* **67,** 8914–8922
30. Liao, H., Hyman, M. C., Baek, A. E., Fukase, K., and Pinsky, D. J. (2010) cAMP/CREB-mediated transcriptional regulation of ectonucleoside triphosphate diphosphohydrolase 1 (CD39) expression. *J. Biol. Chem.* **285,** 14791–14805
31. Rutkowski, D. T., Arnold, S. M., Miller, C. N., Wu, J., Li, J., Gunnison, K. M., Mori, K., Sadighi Akha, A. A., Raden, D., and Kaufman, R. J. (2006) Adaptation to ER stress is mediated by differential stabilities of pro-survival and pro-apoptotic mRNAs and proteins. *PLoS Biol.* **4,** e374
32. Amanso, A. M., Debbas, V., and Laurindo, F. R. (2011) Proteasome inhibition represses unfolded protein response and Nox4, sensitizing vascular cells to endoplasmic reticulum stress-induced death. *PLoS ONE* **6,** e14591
33. Chiribau, C. B., Gaccioli, F., Huang, C. C., Yuan, C. L., and Hatzoglou, M. (2010) Molecular symbiosis of CHOP and C/EBPβ isoform LIP contributes to endoplasmic reticulum stress-induced apoptosis. *Mol. Cell Biol.* **30,** 3722–3731
34. Goodridge, H. S., Reyes, C. N., Becker, C. A., Katsumoto, T. R., Ma, J., Wolf, A. J., Bose, N., Chan, A. S., Magee, A. S., Danielson, M. E., Weiss, A., Vasilakos, J. P., and Underhill, D. M. (2011) Activation of the innate immune receptor Dectin-1 upon formation of a 'phagocytic synapse'. *Nature* **472,** 471–475
35. Lowman, D. W., Greene, R. R., Bearden, D. W., Kruppa, M. D., Pottier, M., Monteiro, M. A., Soldatov, D. V., Ensley, H. E., Cheng, S. C., Netea, M. G., and Williams, D. L. (2014) Novel structural features in *Candida albicans* hyphal glucan provide a basis for differential innate immune recognition of hyphae *versus* yeast. *J. Biol. Chem.* **289,** 3432–3443
36. Tang, Q. Q., and Lane, M. D. (2000) Role of C/EBP homologous protein (CHOP-10) in the programmed activation of CCAAT/enhancer-binding protein-β during adipogenesis. *Proc. Natl. Acad. Sci. U.S.A.* **97,** 12446–12450
37. Zeng, L., Lindstrom, M. J., and Smith, J. A. (2011) Ankylosing spondylitis macrophage production of higher levels of interleukin-23 in response to lipopolysaccharide without induction of a significant unfolded protein response. *Arthritis Rheum.* **63,** 3807–3817
38. Ciccia, F., Accardo-Palumbo, A., Rizzo, A., Guggino, G., Raimondo, S., Giardina, A., Cannizzaro, A., Colbert, R. A., Alessandro, R., and Triolo, G. (2014) Evidence that autophagy, but not the unfolded protein response, regulates the expression of IL-23 in the gut of patients with ankylosing spondylitis and subclinical gut inflammation. *Ann. Rheum. Dis.* **73,** 1566–1574
39. Averous, J., Bruhat, A., Jousse, C., Carraro, V., Thiel, G., and Fafournoux, P. (2004) Induction of CHOP expression by amino acid limitation requires both ATF4 expression and ATF2 phosphorylation. *J. Biol. Chem.* **279,** 5288–5297
40. Bradley, M. N., Zhou, L., and Smale, S. T. (2003) C/EBPβ regulation in lipopolysaccharide-stimulated macrophages. *Mol. Cell. Biol.* **23,** 4841–4858
41. Strasser, D., Neumann, K., Bergmann, H., Marakalala, M. J., Guler, R., Rojowska, A., Hopfner, K. P., Brombacher, F., Urlaub, H., Baier, G., Brown, G. D., Leitges, M., and Ruland, J. (2012) Syk kinase-coupled C-type lectin receptors engage protein kinase C-δ to elicit Card9 adaptor-mediated innate immunity. *Immunity* **36,** 32–42
42. Humphreys, J. M., Piala, A. T., Akella, R., He, H., and Goldsmith, E. J. (2013) Precisely ordered phosphorylation reactions in the p38 MAP kinase cascade. *J. Biol. Chem.* **288,** 23322–23330
43. Arthur, J. S., and Ley, S. C. (2013) Mitogen-activated protein kinases in innate immunity. *Nat. Rev. Immunol.* **13,** 679–692
44. Chooi, K. P., Galan, S. R., Raj, R., McCullagh, J., Mohammed, S., Jones, L. H., and Davis B. G. (2014) Synthetic phosphorylation of p38α recapitulates protein kinase activity. *J. Am. Chem. Soc.* **136,** 1698–1701
45. Canagarajah, B. J., Khokhlatchev, A., Cobb, M. H., and Goldsmith, E. J. (1997) Activation mechanism of the MAP kinase ERK2 by dual phosphorylation. *Cell* **90,** 859–869
46. Hale, K. K., Trollinger, D., Rihanek, M., and Manthey, C. L. (1999) Differential expression and activation of p38 mitogen-activated protein kinase α, β, γ, and δ in inflammatory cell lineages. *J. Immunol.* **162,** 4246–4252
47. Askari, N., Beenstock, J., Livnah, O., and Engelberg, D. (2009) p38α active *in vitro* and *in vivo* when monophosphorylated at threonine 180. *Biochemistry* **48,** 2497–2504
48. Saxena, M., Williams, S., Taskén, K., and Mustelin, T. (1999) Crosstalk between cAMP-dependent kinase and MAP kinase through a protein-tyrosine phosphatase. *Nat. Cell Biol.* **1,** 305–311
49. Blanco-Aparicio, C., Torres, J., and Pulido, R. (1999) A novel regulatory mechanism of MAP kinases activation and nuclear translocation mediated by PKA and the PTP-SL tyrosine phosphatase. *J. Cell Biol.* **147,**

1129–1136
50. Keyse, S. M. (2000) Protein phosphatases and the regulation of mitogen-activated protein kinase signaling. *Curr. Opin. Cell Biol.* **12,** 186–192
51. Farooq, A., and Zhou, M. M. (2004) Structure and regulation of MAPK phosphatases. *Cell. Signal.* **16,** 769–779
52. Waas, W. F., and Lo, H. H. (2001) The kinetic mechanism of the dual phosphorylation of the ATF2 transcription factor by p38 mitogen-activated protein (MAP) kinase α. Implications for signal/response profiles of MAP kinase pathways. *J. Biol. Chem.* **276,** 5676–5684
53. Naqvi, S., Martin, K. J., and Arthur, J. S. (2014) CREB phosphorylation at Ser133 regulates transcription via distinct mechanisms downstream of cAMP and MAPK signaling. *Biochem. J.* **458,** 469–479
54. Gupta, S., Campbell, D., Dérijard, B., and Davis, R. J. (1995) Transcription factor ATF2 regulation by the JNK signal transduction pathway. *Science* **267,** 389–393
55. Baan, B., van der Zon, G. C., Maassen, J. A., and Ouwens, D. M. (2009) The nuclear appearance of ERK1/2 and p38 determines the sequential induction of ATF2-Thr-71 and ATF2-Thr-69 phosphorylation by serum in JNK-deficient cells. *Mol. Cell. Endocrinol.* **311,** 94–100
56. Morton, S., Davis, R. J., and Cohen, P. (2004) Signalling pathways involved in multisite phosphorylation of the transcription factor ATF-2. *FEBS Lett.* **572,** 177–183
57. Wang, L., Payton, R., Dai, W., and Lu, L. (2011) Hyperosmotic stress-induced ATF-2 activation through Polo-like kinase 3 in human corneal epithelial cells. *J. Biol. Chem.* **286,** 1951–1958
58. Fuchs, S. Y., Xie, B., Adler, V., Fried, V. A., Davis, R. J., and Ronai, Z. (1997) c-Jun NH_2-terminal kinases target the ubiquitination of their associated transcription factors. *J. Biol. Chem.* **272,** 32163–32168
59. Khayrullina, T., Yen, J. H., Jing, H., and Ganea, D. (2008) *In vitro* differentiation of dendritic cells in the presence of prostaglandin E_2 alters the IL-12/IL-23 balance and promotes differentiation of Th17 cells. *J. Immunol.* **181,** 721–735
60. Molle, C., Zhang, T., Ysebrant de Lendonck, L., Gueydan, C., Andrianne, M., Sherer, F., Van Simaeys, G., Blackshear, P. J., Leo, O., and Goriely, S. (2013) Tristetraproline regulation of interleukin 23 mRNA stability prevents a spontaneous inflammatory disease. *J. Exp. Med.* **210,** 1675–1684